EUROVOLC

European Network of
Observatories and Research Infrastructure for Volcanology

Deliverable Report

D9.1 Seismic changes as an unrest detection tool

Work Package:	*Volcano pre-eruptive unrest detection schemes*	
Work Package number:	*WP9*	
Work Package leader:	*Chris Bean*	
Task (Activity) name:	*Using seismic tremor as a real-time unrest indicator; Tracking pre-eruptive changes in material mechanical properties; Preliminary modelling of the strain field*	
Task numbers:	*9.1, 9.2 & 9.3*	
Responsible Task leader:	*Chris Bean*	
Lead beneficiary:	*DIAS*	
Author(s)	*Patrick Smith, Mariantonietta Longobardi, Chris Bean* *With contributions from: Tim Sonnemann Kristín S. Vogfjörd Yesim Cubuk Sabuncu, Kristín Jónsdóttir, , Freysteinn Sigmundsson, Carmen Moreno Lopez*	
Type of Deliverable:	*Report [X]* *Prototype [ ]*	*Demonstrator [ ]* *Other [ ]*
Dissemination level:	*Public [X]* *Prog. Participants [ ]*	*Restricted Designated Group [ ]* *Confidential (consortium) [ ]*

Programme: H2020
Project number: 731070

Contents

Summary 1

Introduction 2

1. Development of a real-time tremor analysis tool (RETREAT) for seismic array data 2

Background 2

Overview and method 3

Examples 5

Real-time data 5

Archive data 6

Application to infrasound data 7

Dissemination and feedback 8

2. Towards, real-time automatic array analysis of earthquakes at Hekla volcano in Iceland 9

3. Results from the comparison of seismic wave-velocity changes using CWI 14

Background 14

Method and Results 14

4. Seismic velocity changes in Iceland detected using ambient noise 19

5. Seismic velocity changes at El Hierro, Canary Islands in 2011-2014 22

6. Joint inversion of multiparametric data 26

References 27

Summary

This report summarizes the work undertaken in the development of pre-eruptive unrest detection tools that use seismic changes recorded at active volcanoes.

The **primary focus** is **on developing community tools for tracking tremor and microseismicity**, both on real-time and archived data. Volcanoes can display pre, syn and post-eruptive tremor. One important means of better understanding the processes driving tremor is to track the spatio-temporal evolution of its 3D location. This is best achieved using seismic arrays. A python-based software tool, RETREAT, has been successfully developed that uses seismic array data and array processing techniques to help detect, quantify and locate volcanic tremor signals in real-time. The tool has been tested, in an academic environment, on both real time and archived data. The tool is now ready for testing and implementation in a volcano monitoring setting at observatories, and is also freely available to download, as a EUROVOLC community tool. In addition, a second complementary real-time tool has been developed specifically to detect and track microseismicity at the planned small aperture HEIKSISZ array at Hekla volcano in Iceland. This tool has a slightly different focus to RETREAT, and uses an iterative approach to detect phase arrivals as well as using beamforming to locate signals. Ongoing development in the near future may allow the two tools to be unified and benefit from each other.

A **secondary focus** under this deliverable is **on tracking seismic velocity changes associated with volcanic eruptions**. This has been done using (1) coda-wave interferometry (CWI) on seismic multiplets, (2) analysis of ambient seismic noise, as well as (3) by analysis of an improved earthquake catalogue by using variations in Vp/Vs ratios. CWI applied to multiplets of similar earthquakes recorded prior to the 2018 eruption at Sierra Negra volcano, Galapagos, detected both short and long-term decreases in seismic velocity during the pre-eruptive period. Ambient noise data associated with repeated volcanic intrusions into the Reykjanes volcanic system, on the Reykjanes Peninsula, Iceland during the first half of year 2020 was used to analyze changes in seismic velocity in almost real-time, with cross-correlation functions computed using the MSNoise tool, also revealing a significant decrease in seismic velocity during the unrest period, in general agreement with observed deformation data. Preliminary results from the analysis of Vp/Vs and Poisson's ratios calculated from an improved earthquake catalogue suggest changes in P- and S-wave velocities before and after the 2011 eruptive activity at El Hierro, Canary Islands with, on average, greater Vp/Vs values during the unrest in comparison with the post-eruptive period.

Lastly, the array tracking tools and velocity change studies using only seismic data have been **complemented by a new approach to joint inversion of multiparametric data** that is developing data driven tools to automate the diagnosis of variations of volcanic state in real-time. This study sheds light on what conditions need to be in place in a volcano for an eruption to start, with magma buoyancy as an important factor, and highlights that large eruptions can occur with only minor precursory activity.

A note on this deliverable:

As described in the DoA this deliverable encompasses Tasks 9.1 - using seismic tremor as a real-time unrest indicator; Task 9.2 - tracking pre-eruptive changes in material mechanical properties and Task 9.3 – preliminary modelling of the strain field, as a complement to task 9.2.
Tasks 9.1 and 9.2 have been completed. Task 9.3 is still ongoing as new analysis routines applied to data from the 2014 El Hierro eruption led to a substantial increase in the number of detected events (> 40k), opening a window for additional work on velocity changes (additional work reported here) in task 9.2

In this WP there is significant emphasis on the detection and tracking of seismic tremor as an unrest monitoring tool. Specifically there is an emphasis on the application of small aperture seismic arrays (clusters of 'closely spaced' stations that sit outside the epicentral area of the tremor under investigation). Analysis tools are developed in the WP specifically for real-time analysis of array data.

Whilst it is possible to locate seismic tremor using the amplitudes recorded on 'traditional' seismic networks that encompass the epicentral area of the tremor source(s) (we applied this methodology on Sierra Negra in the Galapagos, as outlined in our previous 18M report), a relatively dense network of 10 or more stations is usually required. This station configuration is generally not available, in part because it would require *a priori* knowledge of the location of future tremor. The advantage of arrays is that they can be used to study both 'nearby' and 'distal' tremor that lies well 'outside' the array, and as they are small in aperture they can often be hard-wired to a central hub for data transmission (essential for real time analysis). Hence **our recommendation is that seismic arrays should be increasingly used as a standard component of the volcano monitoring toolkit** - not only as a research tool, as is currently common practice. We hope that the development of 'easy-to-use' real-time array data analysis tools (like RETREAT, developed here in EUROVOLC) will help encourage the application of real-time small aperture arrays for monitoring purposes.

In this WP we also look at seismic velocity changes in some detail, both using multiples (repeating similar earthquakes) and background seismic noise interferometry. Whilst we do see velocity decrease associated with both unrest (Iceland) and pre-eruption (Galapagos), the interpretation of the physical mechanisms underlying these signals is still an open question that we are continuing to pursue. However from a phenomenological point of view, velocity drops could be viewed with interest as a potential indication of emerging unrest/eruption.

Introduction

The objectives of WP9 are to further develop, test and implement schemes for pre-eruptive unrest detection. These objectives are distinct from and complementary to those of WP8, which deal with syn-eruptive early warning.

Early identification that magma is moving towards the surface is very important for mitigation of volcanic risk, and detection of pre-eruptive unrest is underpinned by continuous real-time monitoring and real-time evaluation of these data. In principle joint real-time analysis and correlation of multi-parameter data can pinpoint pre-eruptive unrest. However, given the potential unrest timescales, from years to minutes prior to an eruption, meaningful automatic multi-parameter pre-eruptive unrest detection is far from trivial in practice.

Here we report on progress to address this challenge by focusing on how seismic changes, particularly seismic tremor and changes in seismic velocity, can be used as a tool to detect pre-eruptive unrest. Here we study both tremor and velocity changes as, in general in observatories around the world, they do not receive the same level of attention as for example (better understood) changes in seismicity rates or moment release,.

1. Development of a real-time tremor analysis tool (RETREAT) for seismic array data

Background

Volcanic tremor is a sustained seismic signal associated with eruptions and is often linked to movement of magmatic fluids in the subsurface. However, it can occur pre-, syn- and post-eruption and signals with similar spectral content can be generated by several other processes (e.g. flooding, rockfalls). Hence one of the best ways of distinguishing between the processes underlying tremor generation is its spatial location and the real time temporal evolution of that location. As tremor cannot be located using classical seismological methods, its source must be determined using alternatives such as amplitude-based techniques or seismic array analysis. Dense, small-aperture arrays are particularly suited for

analyzing volcanic tremor, yet costs associated with installation and maintenance have meant few long-term or permanent seismic arrays in use for routine monitoring. Therefore, to facilitate greater use of arrays in tracking volcanic tremor sources, we translate recent FUTUREVOLC research achievements on our understanding and quantification of pre-eruptive tremor into a usable and transportable tool suitable for a volcano monitoring setting.

Overview and method

Given this context, a REal-time TREmor Analysis Tool (RETREAT) has been developed that uses seismic array data and array processing techniques to help detect, quantify and locate volcanic tremor signals. While primarily intended as a tool for utilizing seismic array data to locate and track volcanic tremor, RETREAT also has the capability to analyze infrasonic array data to track acoustic sources.

The software tool is python-based and utilizes existing routines from the open-source *ObsPy* framework to carry out analysis of seismic array data in real-time. The tool performs either f-k (frequency-wavenumber) analysis, or Least-Squares beamforming (De Angelis et al., (2020)), to calculate the back azimuth and slowness of seismic signals arriving at the array in overlapping time windows, which, as described in e.g. Eibl et al. (2017), can be used to detect and track the location of volcanic tremor sources.

A schematic overview of the software workflow is shown in Figure 1. A GUI and web-based interface, built using the *PySimpleGUI* python module, allows adjustment of highly configurable input parameters (Figure 2). These include options for choosing and configuring the data source, pre-processing, timing and update options as well as the parameters for the seismic array analysis which must be carefully selected for the specific array.

Once configured, the tool fetches chunks of waveform data in real time and updates its output accordingly. On each update the tool returns a choice of the following plots (e.g. Figure 4):

- Array processing results: time series of the slowness and back-azimuth and optionally the relative power [f-k] or MCCM (mean maximum correlation) [Least-squares]
- Seismic waveform
- Root-Median-Square envelope
- Spectrogram
- A histogram representing the relative power as a function of back-azimuth and slowness in polar form
- An optional plot of the array transfer function
- An optional map of the array and its surroundings, with the calculated back azimuth overlaid.

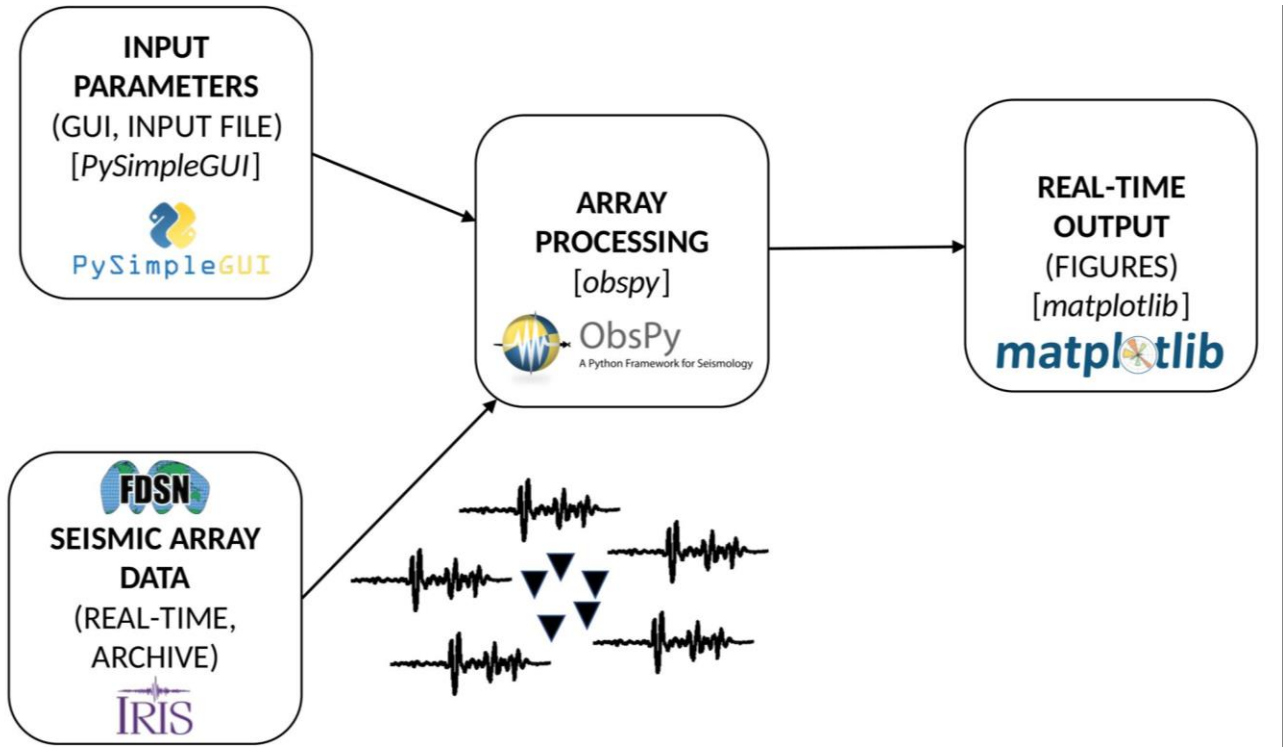

Figure 1. Schematic overview of the RETREAT software package. Input parameters and configuration are collected from the GUI or web interface that was built using the PySimpleGUI module. Next, these settings allow seismic array data (real-time data from external sources, e.g. IRIS or any other server, or existing archive data) to be processed and analyzed using the standard array processing routines in ObsPy. Output figures displaying the results of the array analysis are then produced using the matplotlib python module and are continuously updated as new data is processed.

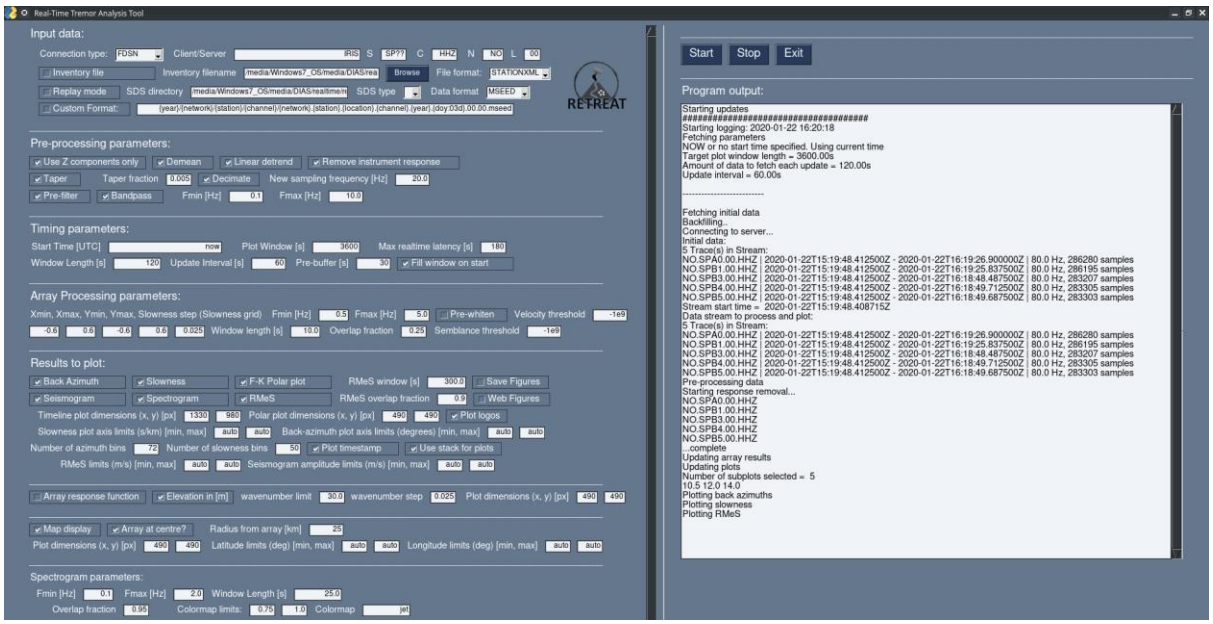

Figure 2. Example screenshot of the GUI interface for the RETREAT tool, showing configurable input parameters and program output window.

Examples

Configuration files and data to run processing of two examples, of real-time and archive data, are included with the distribution. In the original description of this deliverable it was envisaged that array data from Merapi would be used to develop and test the scheme. However it transpired that these data are not available in real time and hence we opted to use real-time data from the small-aperture SPITS seismic array as a development and demonstrator dataset for real time applications. Archived data from the FUTUREVOLC database are used to develop and test the application of this tool on archive data.

Real-time data

As we currently do not have any real time seismic array data from a volcano available within the EUROVOLC project or its partners, the tool has been tested using both the FDSN and SeedLink clients of ObsPy to fetch data from the IRIS datacenter, using example real-time data from the small-aperture SPITS seismic array (Gibbons et al., 2011) in Spitsbergen, Svalbard, as shown in Figure 3. This small-aperture array comprising nine stations is part of the larger NORSAR array, but with an aperture of around 1 km is more typical of the size and characteristics of seismic arrays deployed in volcanic environments.

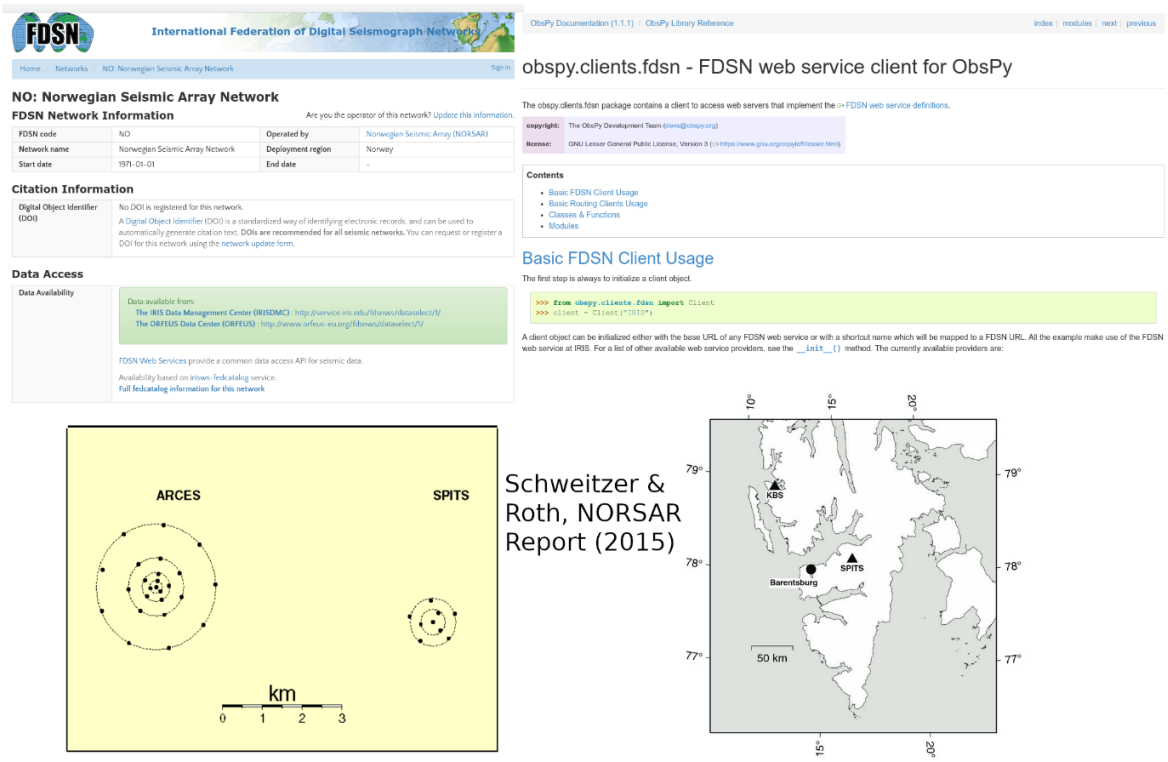

Figure 3. Details of the small-aperture SPITS array, part of the larger NORSAR array, used for testing the software with real-time data. Acquisition of the real-time data stream is via obspy's FDSN client.

An example of the output produced by analyzing real-time data from the SPITS array is shown in Figure 4, displaying: time series of the back azimuth and slowness, the seismogram, spectrogram and envelope; a polar representation of the array processing results and a map showing the projected back azimuth and location of the array.

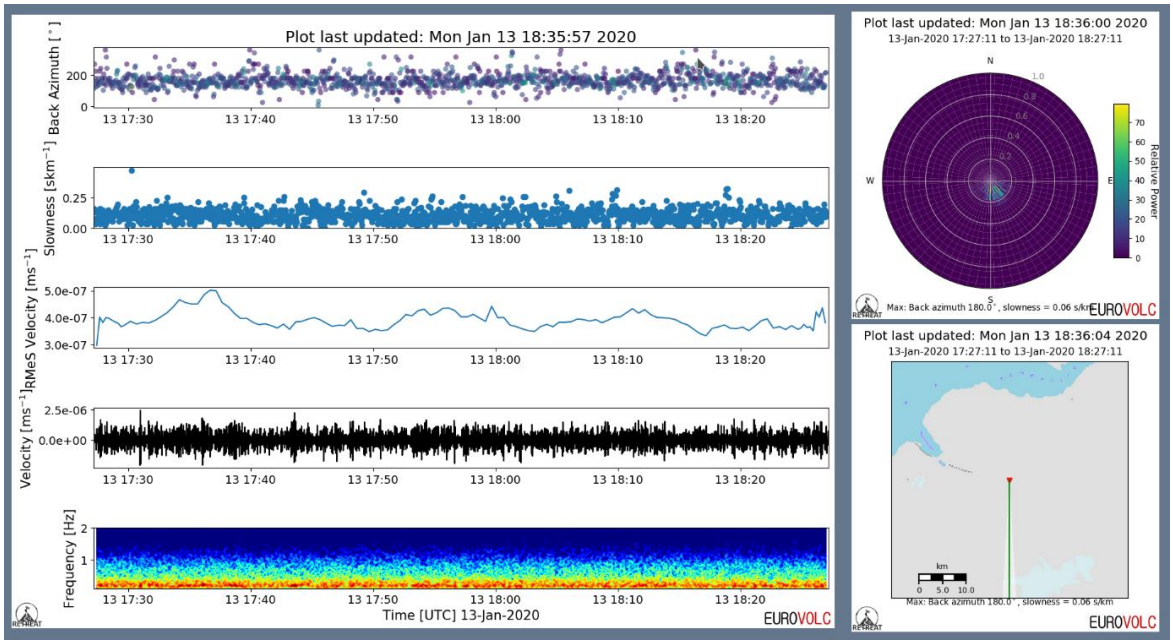

Figure 4. Example of the output figures produced by the RETREAT software tool, showing time series of slowness and backazimuth calculated from f-k analysis, alongside the seismic waveform, envelope and spectrogram and a polar representation of the array processing results. Also shown is a map of the area surrounding the SPITS array, with the resulting back azimuth overlaid.

Use of other real-time data sources that are supported by ObsPy (e.g. ArcLink, Earthworm, Winston servers) will be considered and/or further developed depending on need.

Archive data

A 'replay' mode using existing archive seismic array data has also been implemented to allow analysis of non-real-time datasets. Figure 5 shows archive data from the 2014 eruption at Holuhraun and Bárdarbunga volcano in Iceland, collected as part of the FUTUREVOLC project (Eibl et al., (2017)):

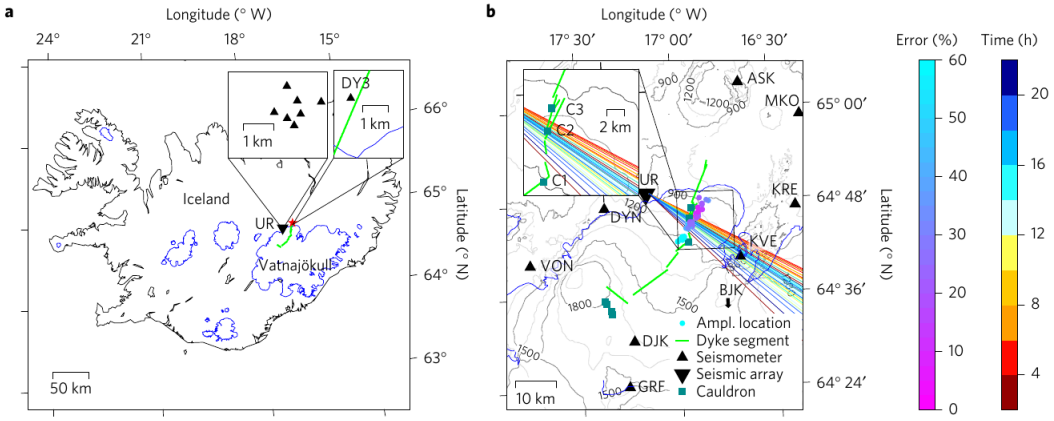

Figure 5. Map of the 7 station UR seismic array deployed as part of FUTUREVOLC to collect data during the 2014-2015 eruption at Bardarbunga volcano in Iceland. The location of the erupted lava flow field in Holuhraun is indicated with a red star, and the approximate propagation path of the dyke intrusion below the glacier by the green line. The right-hand panel shows the temporal evolution of the pre-eruptive tremor location estimates determined from the array analysis (from Eibl et al., (2017)).

Example results from analysis of data on 03 September 2014 using the RETREAT software are shown in Figure 6, corresponding to part of the same time period analyzed in Eibl et al., (2017). Results using RETREAT show an excellent match with the previous analysis.

Several hours of data from the UR array between 00:00 and 08:00 UTC on 03 September 2014 are included with the distribution, corresponding to part of the time period analyzed in Eibl et al. (2017). Example results of the analysis of these data using RETREAT are shown in Figure 6. The configuration for this example closely follows the parameters used by Eibl et al. (2017), with the data from the seven station array filtered between 0.8 and 2.6 Hz after being downsampled to 20 Hz. The time period analyzed represents pre-eruptive tremor prior to a suspected sub-glacial eruption, based on observed cauldron formation approximately, 12 km from the UR array. The tremor signal is centered around 1.3 Hz, with harmonic overtones at 0.25 Hz spacing, and the upper end of measured slowness values of 0.6-0.75 skm^{-1} from the array analysis support a strong surface wave component. Array analysis and location of the tremor signal, along with mapping of the slowness changes to depth changes by modelling the tremor as a comb function, is interpreted by Eibl et al. (2017) as the tremor representing microseismicity resulting from brittle failure in the weak uppermost crust, marking the onset of shallow dyke formation.

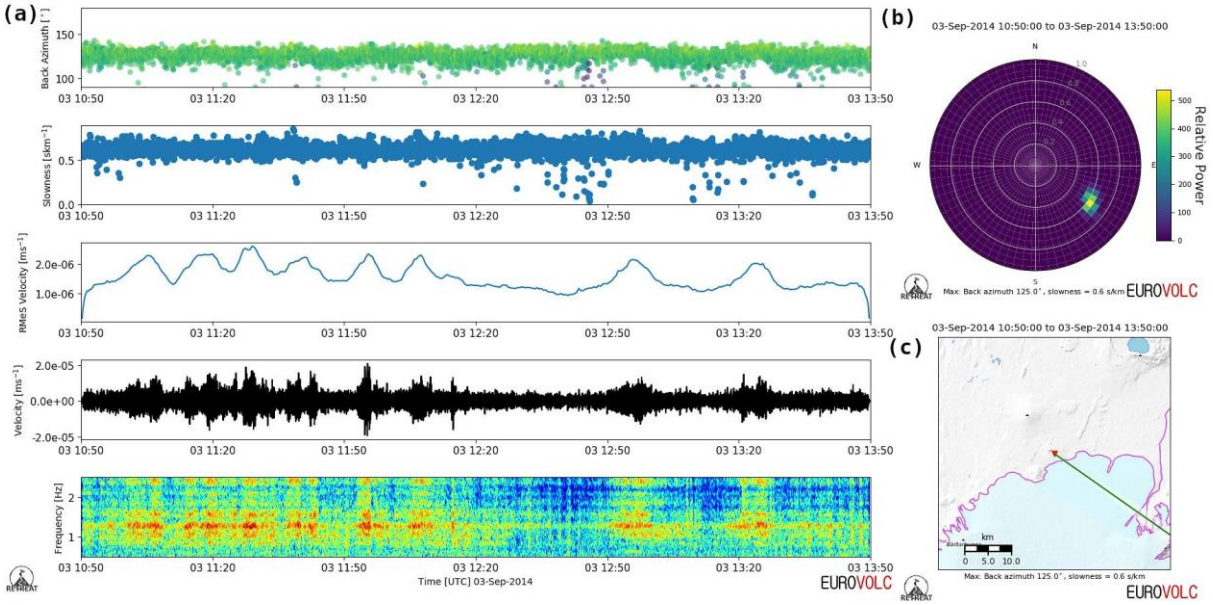

Figure 6. Output figures produced by the RETREAT software for the archive data example. (a) Time series of slowness and backazimuth calculated from f-k analysis, alongside the seismic waveform, envelope and spectrogram and (b) a polar representation of the array processing results are displayed. Also shown in (c) is a map of the area surrounding the UR array, with the resulting back azimuth overlaid, closely matching the results found by Eibl et al., (2017).

Application to infrasound data

In a similar manner to seismology, as well as more widely distributed networks, tight clusters of stations or small aperture arrays of infrasound sensors have been used extensively to monitor and track the location of sub-aerial volcanic phenomena, such as explosions, gas and ash emission, dome or sector collapses, pyroclastic density currents and lahars.

Although designed specifically for seismic array data (with a particular focus on volcanic tremor), RETREAT can also be applied to data from an array of infrasound sensors, using f-k analysis in the same way as for seismic data to retrieve the azimuth and slowness of infrasonic acoustic waves arriving at the array. However, due to the lower velocity of acoustic waves compared to seismic waves (and therefore higher slowness – up to 3 s/km and beyond), a larger slowness grid is required for the analysis, which is far less computationally efficient and results in significantly longer processing times.

With this in mind, RETREAT also contains a python implementation of a time-domain Least-Squares inversion method that uses cross-correlation to compute time delays between station pairs to carry out the beamforming and derive an estimate of the apparent horizontal velocity. This method (Olson and Szuberla, 2005; Haney et al., 2018) is also applied on a series of overlapping sub-windows to produce time series of the back azimuth and slowness, and has the advantage of being faster to compute, while developments by De Angelis et al. (2020) also allow for direct estimates of the uncertainties of these measurements. It also returns a time series of the mean cross-correlation maxima (MCCM), which by choosing a certain threshold can be a useful parameter for event detection, or even alarm triggering.

In order to illustrate the capability of RETREAT to analyze infrasonic array data in addition to seismic data, Figure 7 shows a comparison between the two beamforming methods. The data analyzed are from a 2019 deployment of two 6-sensor infrasound arrays at Mt. Etna in Italy, and are exactly the same as those analyzed and presented in Figure 4 of De Angelis et al. (2020), containing 35 minutes of data from 2 July 2019 at the ENEA array, approximately 1 km to the NW of the summit. The dominant activity is from deep intra-crater explosions at the more southerly Bocca Nuova crater (~145º), occurring consistently across the time series, with a brief interruption from a larger ash-rich explosion at the North East Crater (~110º) at around 10:06 UTC. Data are pre-processed by filtering between 0.7 and 15 Hz, and a 10 second window with 50% overlap is used. The results of the analysis in Figure 7 show that both methods are capable of reproducing the results of De Angelis et al. (2020) and resolving the change in location of activity at around 10:06 UTC; however the Least-Squares method is much faster, which is a key advantage for real-time applications. This method also produces more tightly clustered values, particularly in slowness, and with a step of 0.05 skm^{-1} in the slowness grid limiting the resolution, the f-k analysis takes around two orders of magnitude longer to complete than the Least-Squares inversion.

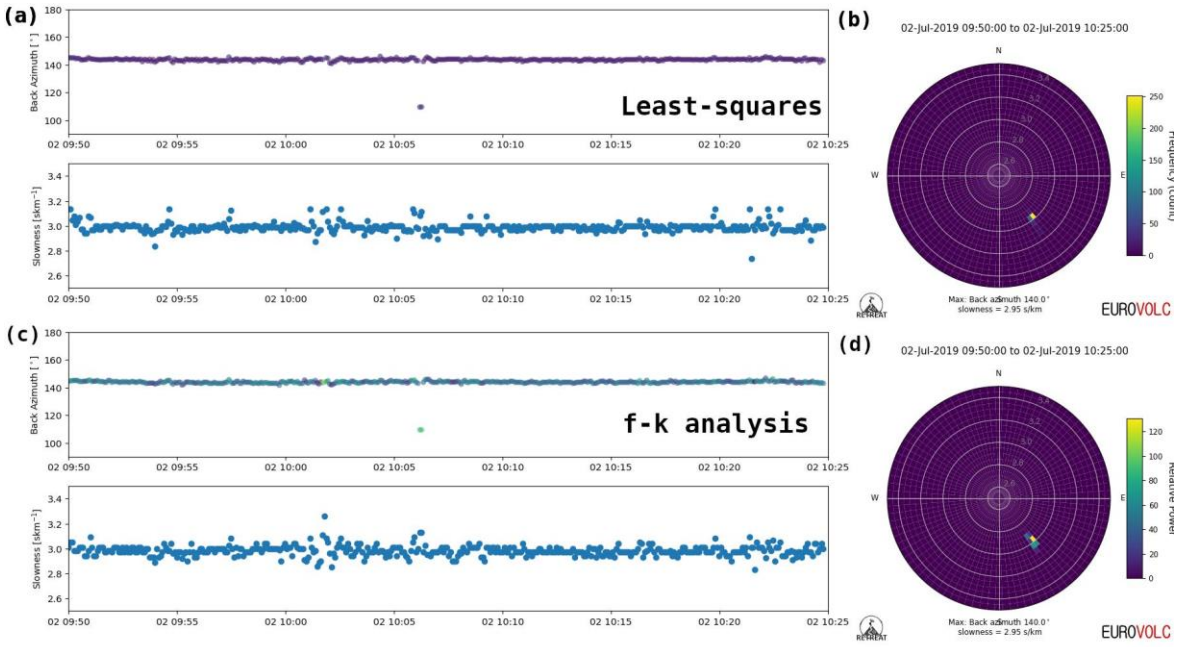

Figure 7. Comparison of RETREAT applied to infrasonic array data using two different beamforming methods. (a) Timeseries of backazimuth and slowness values derived using Least-Squares inversion and (b) corresponding histogram of slowness and backazimuth values in polar form. Note that this is weighted by the MCCM (mean cross-correlation maxima) rather than the relative power as in the f-k case. (c) Timeseries of backazimuth and slowness values derived using f-k analysis and (d) the corresponding histogram of slowness and backazimuth values, weighted by the relative power.

Dissemination and feedback

An open-source publication describing the software has now been published in the journal Frontiers in Earth Science (Smith & Bean, 2020), and the tool has also been made publicly available to download

as a EUROVOLC community output. Development and documentation of this tool are complete, but additional testing using other data sources and volcanic tremor examples are ongoing to improve its usability. The software and documentation is being hosted on the DIAS gitlab page: https://git.dias.ie/paddy/retreat, in a similar manner to the ELM (Elastic Lattice Method) software package as part of WP23, and it is also linked to via the EUROVOLC website and the EUROVOLC wiki page, https://eurovolc.cp.dias.ie/index.php/Open_software

There are plans for a trial implementation at IMO for future array data from Hekla/Katla, and additionally other researchers at other European institutes have also expressed interest in trialling the software at array installations.

2. Towards, real-time automatic array analysis of earthquakes at Hekla volcano in Iceland

One of IMO's aims in WP9 was to implement automatic array analysis of real-time datastreams from a planned small-aperture (1.5-2 km) seismic array, HEKSISZ, near Hekla volcano in Iceland in order to track microseismicity under the volcano in real-time and create capability for pre-eruptive warnings for the volcano. Sudden increase in microseismicity is a common pre-eruptive indicator at Icelandic volcanoes and has been observed prior to all recent eruptions in Hekla. However, the time of first detection of such seismic swarming prior to Hekla eruptions is only around 2 hours, requiring no latency in data transmission and fast performing software delivering results of reliable accuracy. The expectations from such real-time array processing software is the capability to track and map the propagation of microseismicity at the front of a propagating magma intrusion, from the magma storage at >15 km depth under Hekla (Ófeigsson et al., 2011; Geirsson et al., 2012) towards the surface to a fissure eruption along the volcano's axis. The goal is to create readily usable algorithms for continuous real-time analysis of the recorded seismic signals on the array, which are intended to supplement the RETREAT software package of DIAS.

Installation of the HEKSISZ array was planned for summer 2019 under a nationally funded research project. Operational testing of the initially planned location, around 7 km south of the volcano however turned out to be suboptimal with respect to transmission reliability, so a more feasible location 5.5-7.5 km northwest of the Hekla was chosen. However, due to elevated volcanic hazard on the Reykjanes peninsula in Iceland during most of 2020 and other disturbances and confinements caused by COVID-19, the installation at the new site was further delayed until summer 2021.

The first version of a software package for automatic array analysis has been developed at IMO, but with the HEKSISZ array not yet installed testing of the array analysis on earthquakes at varying depths under Hekla is not yet possible. Instead, the software is being tested on data from an existing 12 element, small-aperture strong-motion array, ICEARRAY1, located 75 km west of Hekla in the town of Hveragerdi, in the South Iceland Seismic Zone (SISZ) (Figure 8). A large number of aftershocks at hypocentral distances of 2.5 to 15 km from the array were recorded following a M_W6.3 event in the SISZ in 2008.

The challenge is to detect seismic sources, such as tectonic events, hybrid events and tremor, while also estimating the source location and timing. Detection is accomplished by moving window, multiband frequency-wavenumber (fk) analysis, using both vertical and horizontal components. An iterative process first determines whether a P-wave can be assumed to have arrived by beamforming, according to a specified list of backazimuths, slownesses and frequency bands. For Hekla volcano, the list will account for the azimuthal range of Hekla as seen from the HEKSISZ array, the expected slowness range of phases from events at various depths under the volcano and the expected frequency contents of those dominant phases. A more precise evaluation follows by fk-analysis of the signals. Rotated horizontal components are then processed in order to also detect an expected S-wave. If both P and S waves are

detected, a possible location is projected by using the P-wave's horizontal direction, the incidence angle, the P-S arrival time difference and a local velocity model. Strong velocity gradients and heterogeneities near the surface however can cause significant uncertainties, which may require further evaluation.

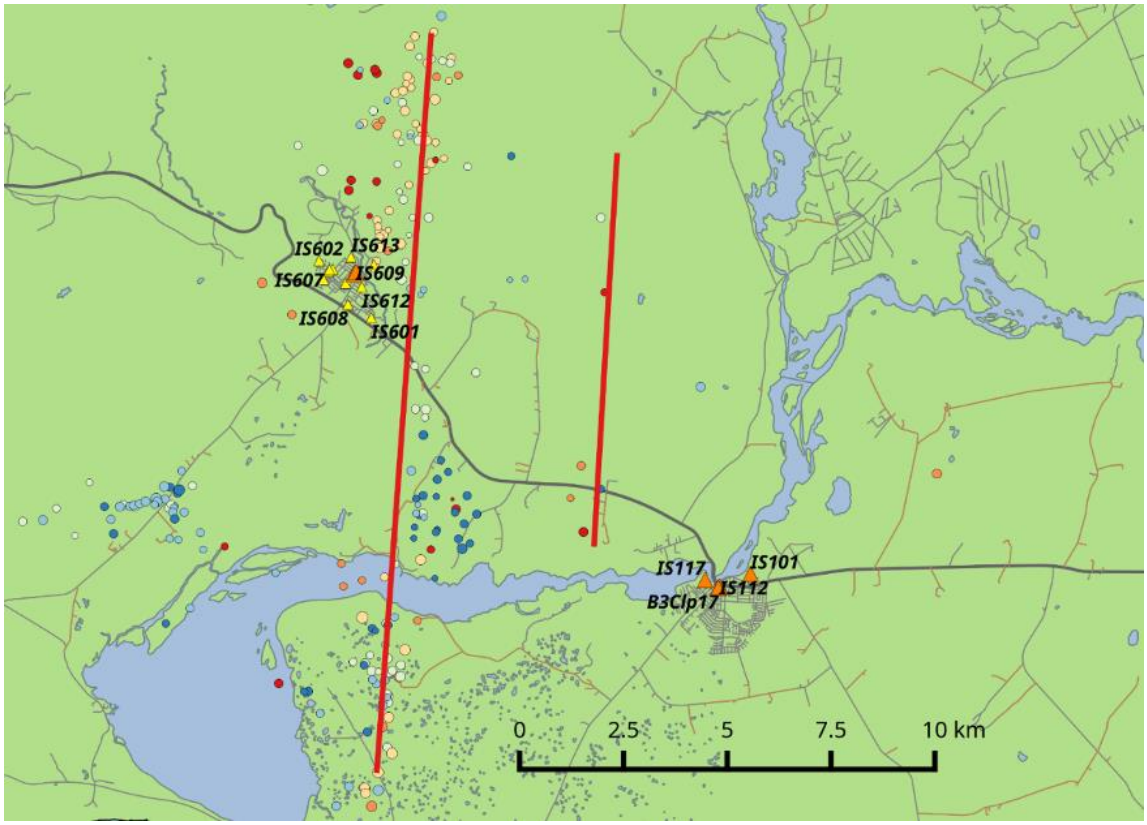

Figure 8. Map showing a view of the ICEARRAY1 stations used to test the algorithm (yellow triangles in upper left quadrant) in the town of Hveragerdi, other seismic stations (orange triangles), the main faults of the 29 May 2008 M_w6.3 earthquake (red lines) and aftershock locations (colored circles).

The electronic software package is free, open-source software written mostly in Python, using the ObsPy package and incorporating a few added C language functions, such as the delayed recursive STA/LTA algorithm developed at NORSAR (New Manual of Seismological Observatory Practice, NMSOP Ch. 9.6), which is used as part of the detector. The software's current technical limitations are the non-complete selection of data formats and lack of a full graphical user interface. To improve these issues, the work done for the RETREAT software will be very useful as the more extensive data handling functions and graphics do not need to be done twice, but instead the two packages can be mostly unified and benefit from each other. Further development in the near future can accomplish these necessary functionalities.

Scientifically, the assessment of source location uncertainty requires more attention as it is currently based on a simple estimate of the half-width of the fk spectral peak and a single 1D velocity model. Further improvements are expected, specifically the combination of array data with data from other near-by single stations, and the combination of multiple arrays if they become available. A future addition might be a machine learning component to categorize the nature of received signals. As mentioned before, seismic sources tend to fall into various different categories and automatically identifying them is challenging but probably within reach of such future enhancements. Synergy with another IMO project targeted to that end and using deep learning is currently at a discussion stage.
Examples of the analysis are shown in Figures 9 and 10, which demonstrate an application of the software to near-source array data analysis and preliminary results. As previously mentioned, the analyzed data are from the 12 element, small aperture ICEARRAY1 in Hveragerdi, which recorded many small aftershocks of the 2008 earthquake at hypocentral distances of 2.5 to 15 km from the array. Figures 9 and 10 show the results of the analysis for one, M1.5 event located 2.3 km NE of the array.

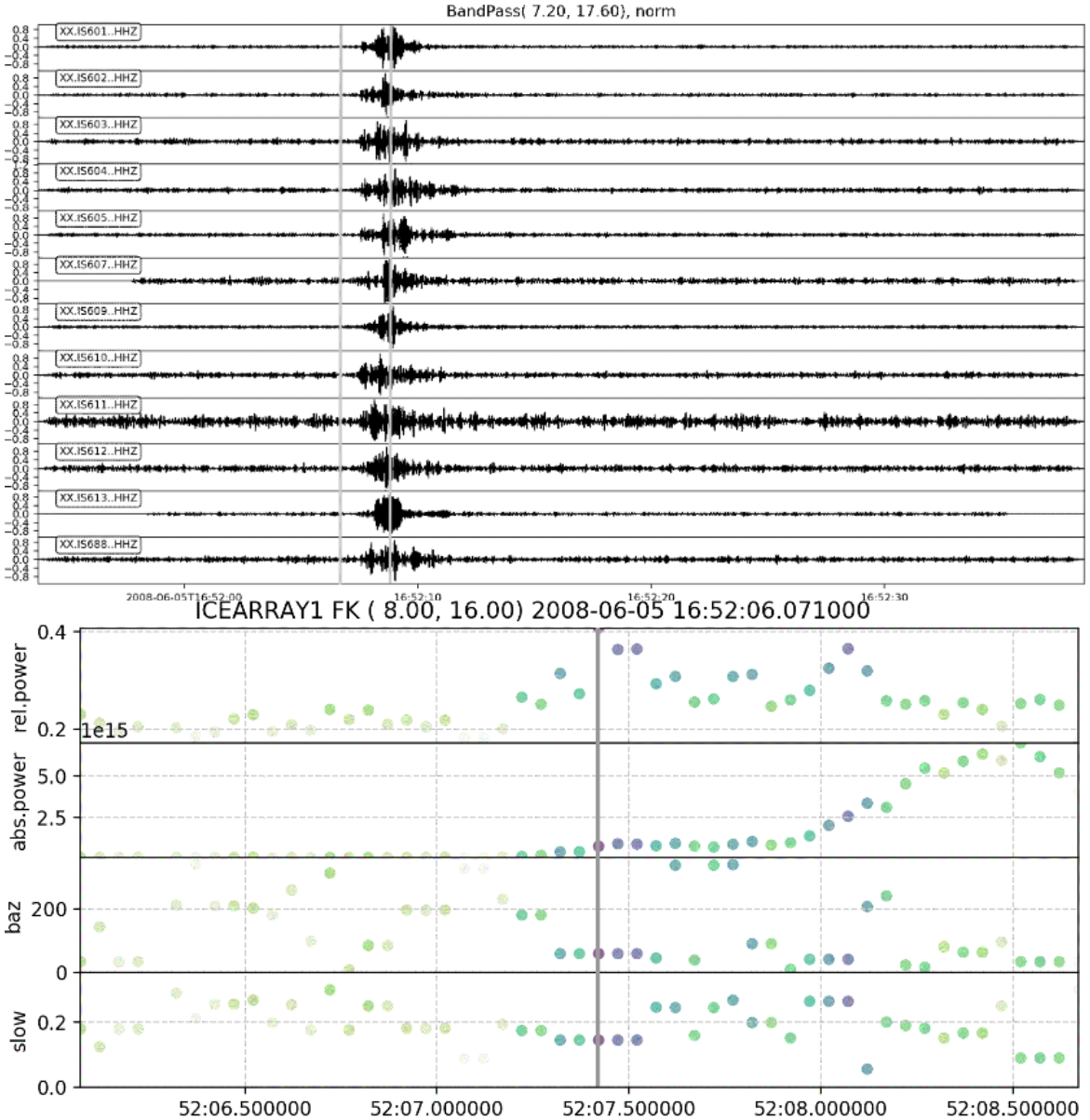

Figure 9. (Upper) Band-pass filtered (7.2-17.6 Hz) vertical component seismograms from a M1.5 aftershock of the M_W6.3 event in 2008, recorded on all ICEARRAY1 stations are shown, with amplitudes normalized by their maximum value. The event is at 2.3 km distance NE of the array. Grey vertical lines indicate the start and end of the 2 s time window used for the fk analysis. (Lower) The four different parameters resulting from the fk analysis within the frequency band 8 – 16 Hz. The vertical gray line indicates the relative beam power, absolute beam power, backazimuth and slowness estimates for the wave arriving within the time window shown in the upper figure. Relative beam power is a measure of signal coherency, meaning a beam formed with that particular slowness retains a given fraction of the sum of all individual sensor signal powers. At perfect constructive interference by all signals, no signal power is lost, and the relative power would be 1.0, while lower values indicate beam signal loss due to destructive interference.

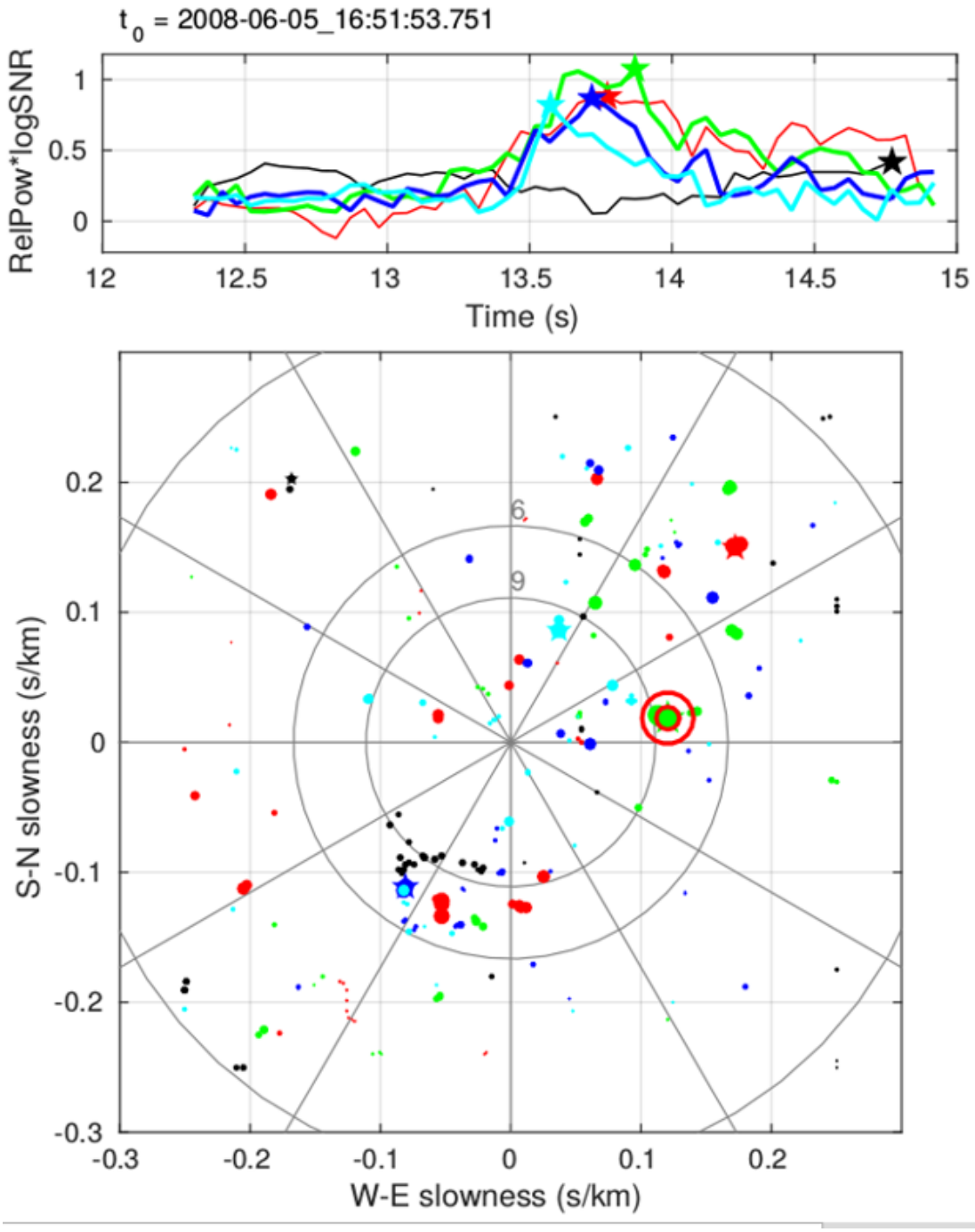

Figure 10. (Upper) High peaks of relative power times log SNR (Qfk) for five different frequency bands indicate a possible P-phase onset. (Lower) [EW, NS] slowness values are shown, scaled by the signal quality measure Qfk. The maximum quality value of each frequency band is represented by a star symbol, while red circles indicate maxima of Qfk > 0.99. Here, the theoretically expected back azimuth was 54 degrees. However, a secondary phase after a weak P-onset caused the peak at medium frequencies (green) to appear at a different azimuth than expected, while a higher frequency band (cyan) shows the earliest clear peak at the actual P-onset time with a backazimuth of about 25 degrees from north. This shows some of the challenges in analyzing small earthquakes in a very heterogeneous crust.

To examine the location accuracy, an automated analysis using the algorithms is compared to independently detected and located earthquakes by the IMO using the SIL network and analysis system. Five different frequency bands were chosen, and it was found that the optimal frequency band for detection and location depends on depth, distance and size of the earthquakes. For the ICEARRAY1 dataset, the bands 10 – 20 Hz and 15 – 30 Hz performed well, due to the proximity to the array and

small size of the tectonic aftershocks. The results are shown in Figure 11. Only azimuthal differences are shown, as the absolute locations have not been estimated using the array. The results apply to the tested events, which are all tectonic events of short duration, mostly on pre-existing faults in the SISZ, whereas the events under Hekla volcano are generally not on single lineaments and their frequency content reflects longer duration source-time functions and higher attenuation in the Eastern Volcanic Zone region around Hekla. Therefore, different frequency bands may be optimal for the HEKSIZ array analysis. Finally, very close events can render the S-wave detection too uncertain to allow meaningful absolute locations, however a more advanced approach is being investigated. The complex geology under ICEARRAY1 consists of alternating lava and sediment layers with many fractures which further decreases location accuracy.

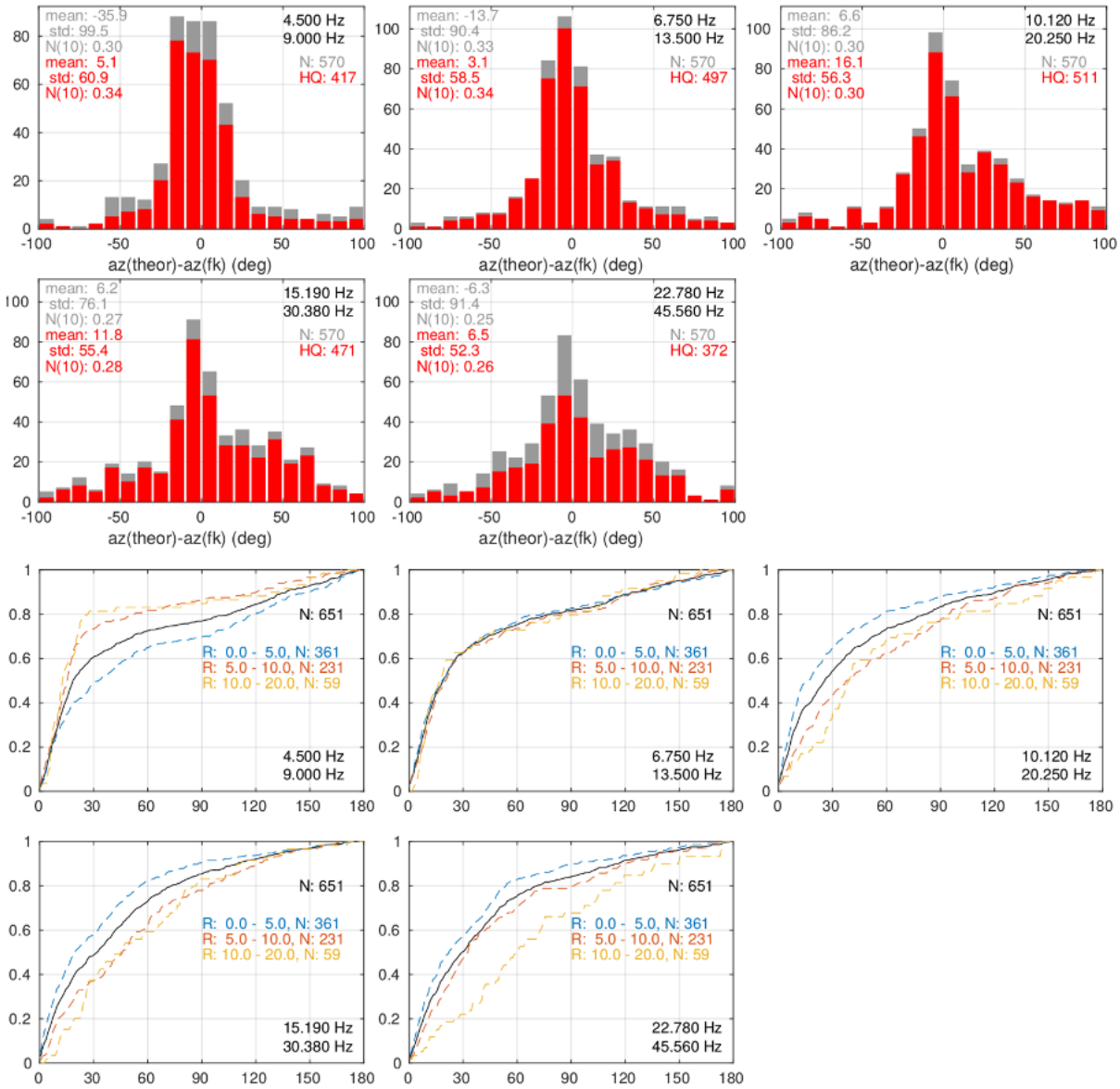

Figure 11. (Upper) Histograms of the difference between single event locations (theoretical azimuth) and fk-based azimuth measures (mismatch) using five different frequency bands for analysis. Red bars show only events that were measured with at least 7 stations, while grey bars indicate all events including those measured with fewer stations. The numbers of such events are indicated by a grey 'N' for the entire dataset, and a red 'HQ' for the high station number events only. The full-dataset (grey) and filtered-dataset (red) values for the mean and standard deviation of mismatch are given as well. The fraction of events with a mismatch of 10 degrees or less is indicated by 'N(10)'. (Lower) Cumulative absolute azimuth mismatch in degrees for five different frequency bands, with solid black lines indicating the combination of all events, while the dashed lines represent events grouped by epicentral distance (R, in km) to the array center. Note that very close events are better located using

higher frequencies (80% have less than 60 degrees mismatch at bands from 10 to 45 Hz), while farther away events require lower frequencies to be reliably resolved (80% of events beyond 10 km distance have less than 30 degrees mismatch only below 9 Hz).

3. Results from the comparison of seismic wave-velocity changes using CWI

Background

This task consists of quantifying how changes in the external stress state and fluid content alter the mechanical properties of an elastic medium, and hence its seismic wave velocity.

Hence, variations in seismic wave velocity can be used as proxies for changes in stress and possible fluid ingression. Temporal variations in seismic wave velocity have previously been monitored and observed prior to volcanic eruptions. In the absence of additional constraints related to stress or fluid changes on the volcano, these pre-eruptive changes are difficult to interpret and hence the causes of them are usually not well understood. Hence while tracking velocity changes may be informative, tracking tremor location is of significantly greater practical value in terms of unrest detection, which is why tremor discrimination is the primary focus of D9.1.

Coda Wave Interferometry (CWI) is used to measure time-lapse changes in seismic velocity on seismic multiplets (repeating similar earthquakes). In particular, we focus our analysis on using this technique to calculate velocity changes using data recorded prior to the 2018 eruption of Sierra Negra volcano, Galapagos Island. Other EUROVOLC work (deformation) has also been undertaken on this volcano, which influenced its choice.
Sierra Negra is a large basaltic shield volcano, located on the island of Isabela in the Galapagos Islands, Ecuador. It is one of the most active volcanoes in the Galapagos Islands and prior to 2018, it last erupted in 2005. Since 2016 the volcano has shown elevated rates of seismicity and ground deformation. The rates increased further in October 2017, to 20 cm/month and hundreds of detected earthquakes per day, raising concerns about a possible eruption in the near future. On 26th June 2018 an intense seismic swarm started at around 17:15 UTC. Seismic tremor dominated at about 19:45 UTC, which marked the onset of the eruption. A very large seismicity sequence preceded the eruption. Our aim is to understand whether changes in seismic velocity, measured using CWI applied to multiplets, can provide new insight into the physical processes related to the eruption. If velocity changes can be detected, there is an excellent seismic network at this site in addition to a GPS network which can help constrain the deformation field.

Method and Results

Coda Wave Interferometry (CWI) is a technique which exploits the sensitivity of coda waves to small changes in the velocity, by comparing the coda of repeating earthquakes (Snieder 2006). Repeating earthquakes are defined as events that have ‘the same’ location (i.e. events less than seismic wavelength/4 apart) and very similar focal mechanisms. Because of multiple scattering, the coda part of seismograms represents wavelets scanning the medium over long path lengths, and hence is very sensitive to the structure of the medium. By looking at repeating seismic events with the same location and source properties, the scattering medium is considered as the interferometer that allows detailed measurements of velocity changes in the medium. Here the correlation coefficient of pairs of seismic traces are compared in the time domain in order to first identify families of repeating events. As mentioned above there was a large pre-eruptive seismicity field, and many of these earthquakes have similar seismograms. However for CWI to work the repeating waveforms must have correlation coefficients > 0.85 (say), and unfortunately, despite high levels of seismicity, initially we found very few events that satisfy this strict criterion. The high levels of pre-eruptive seismicity followed by ‘loud’

tremor makes it difficult to find 'clean' repeating events in the data stream using traditional methodology.
Hence we have recently adopted a new tool in the search for multiplets, the REDpy (Repeating Earthquake Detector in Python) tool (Hotovec-Ellis and Jeffries, 2016).
This detector begins by using an STA/LTA algorithm to identify event arrivals on different channels across a seismic network and stores events in a series of tables, just as with typical detection algorithms. The difference between REDPy and other tools is in the event association step. When enough stations or channels are triggered at once, an event is run through a series of cross-correlations in the frequency domain for comparison with other events in the catalogue and assignment based on cross-correlation coefficient values (Figure 12).

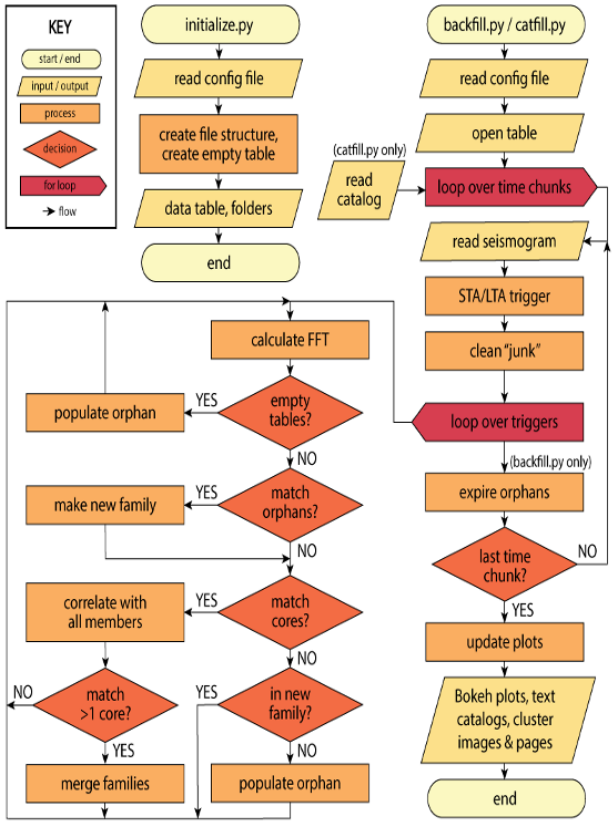

Figure 12. REDpy - Basic Logic.

We applied the CWI technique on the similar waveforms detected. The computation is performed using the cross-correlation in different window lengths and using those independent estimates to quantify velocity variations and associated errors through a mean least square. Under the hypothesis of a uniform velocity variation, the plot of lag-time corresponding to the maximum of the cross-correlation per time window versus time shows a linear relationship, where the mean velocity perturbation is proportional to the slope. We show a multiplet pair in Figure 13 and the application of CWI technique to this pair. We apply the CWI method to multiplets with a cross-correlation of at least 0.9 in the time interval 25/05/2018 to 26/06/2018.
The CWI analysis was performed entirely using a program specifically written in Matlab, where it is possible to interactively handpick the first arrival, align the traces, check the onset and then compute the changes from the plot of the maximum of the cross-correlation per time window versus time. A linear variation of the lag-time reflects velocity changes while if the plot is constant in time, source or scattering movement can be detected by studying the variation of the variance of the perturbation. We use each event pair to both determine the percentage change in velocity between the events in the pair and to determine the sign of the change, faster or slower.

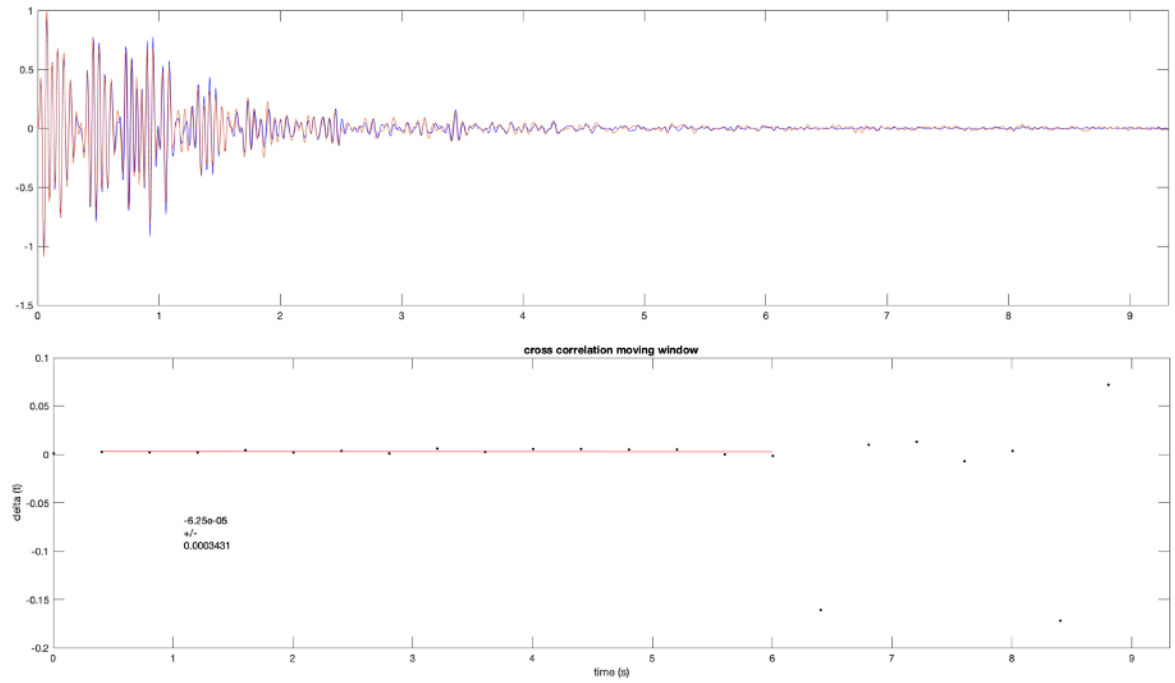

Figure 13. Top: visual comparison of the early part and coda for the multiplets detected on 30/05/2018 (blue) and 23/06/2018 (red). Bottom: CWI analysis. The seismograms were first aligned at the P-onset; the time-shifted cross-correlation was then computed for non-overlapping windows (the length of the window is 6 cycles). The velocity variation can be retrieved from the slope of the time vs lag-time. The slope has been computed up to 6s. The gap at 7s is related to a sudden drop in cross correlation, due to a spike in one of the seismograms of the pair. The velocity variation and its associated error are computed by mean least squares.

We analysed data recorded from May 25th to June 26th 2018 at six stations, which are part of the Sierra Negra IGUANA temporary network (primarily DIAS instruments with IGUANA coordinated from the University of Edinburgh) Figure 14.

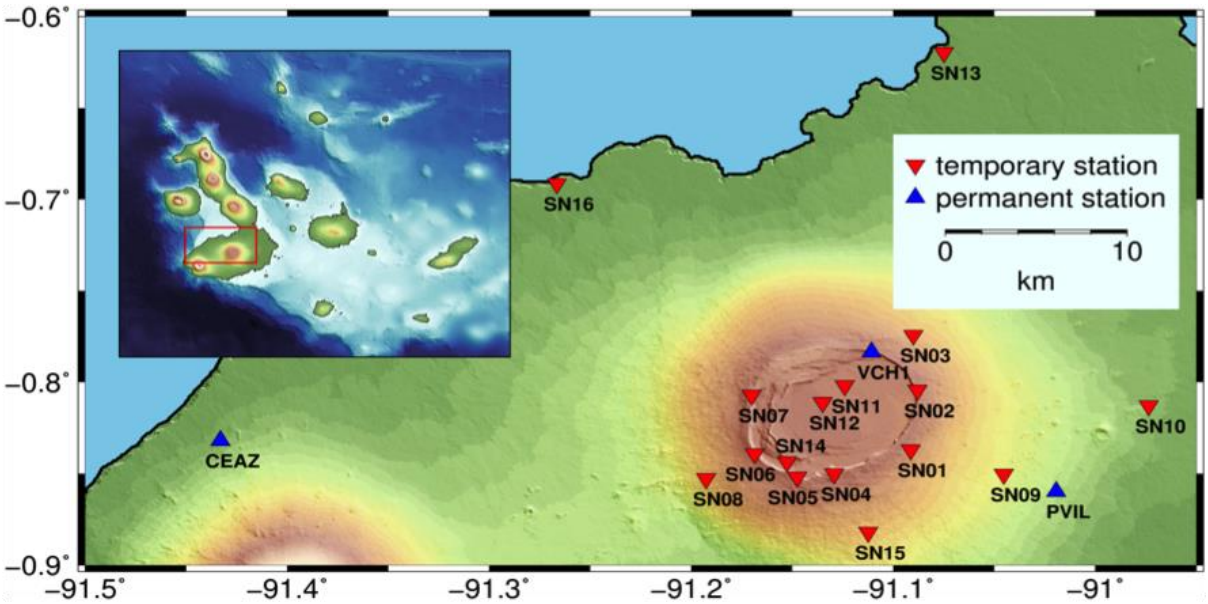

Figure 14. A map of the seismic network used in this study. Inset indicates the location of Sierra Negra and Isabela island within the Galapagos Islands.

REDpy detected more than three hundred repeating earthquakes grouped in more than 100 clusters (Figure 15). We applied the CWI method to the events occurring 3-4 weeks apart. We show some example of CWI applied to events recorded at SN04 station (Figure 16).

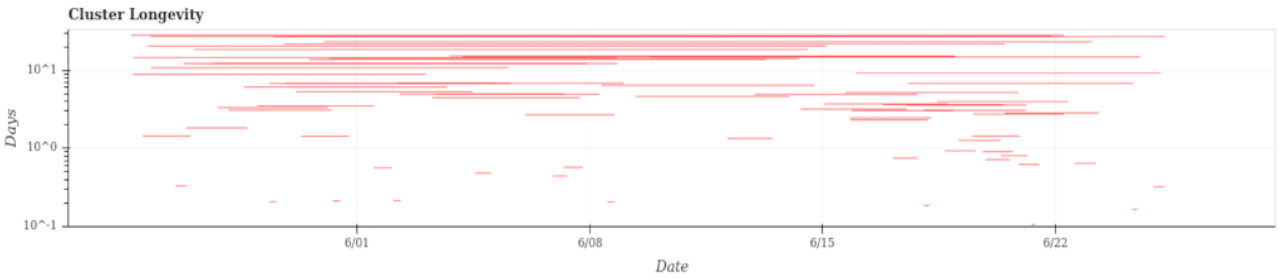

Figure 15. Cluster Longevity for events detected from 25/05/2018 to 26/06/2018. The clusters are ordered in the occurrence timeline by the length of time they are active. This can be useful for identifying times when many clusters stop or are created.

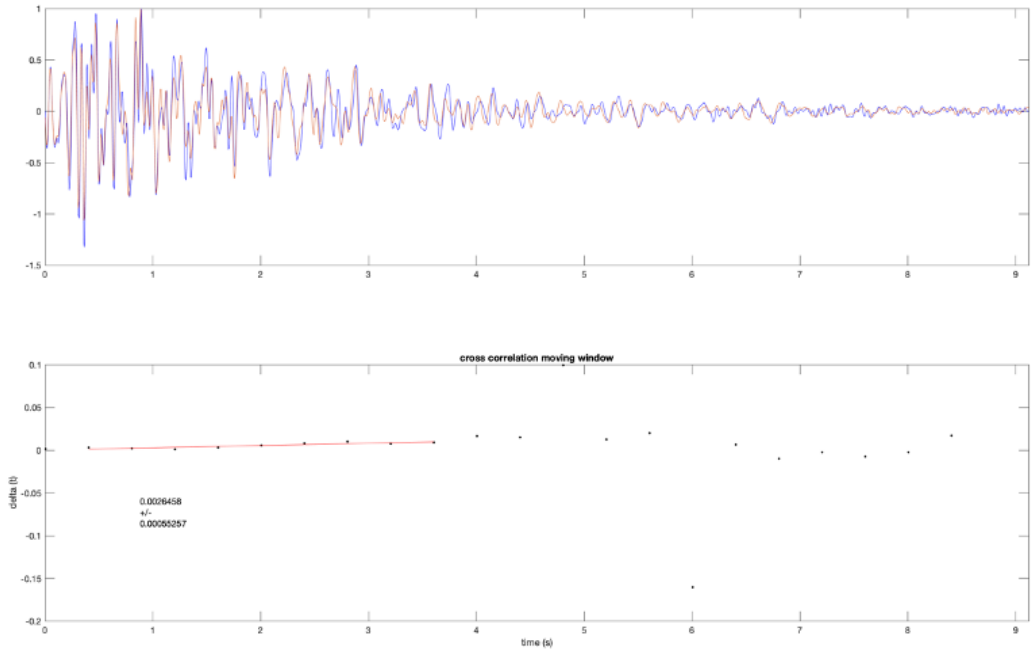

Figure 16a. Top: visual comparison early part and coda for the multiplets detected on 25/05/2018 (blue) and 22/06/2018 (red), SN04 station. Bottom: CWI analysis. The velocity variation can be retrieved from the slope of the time vs lag-time.

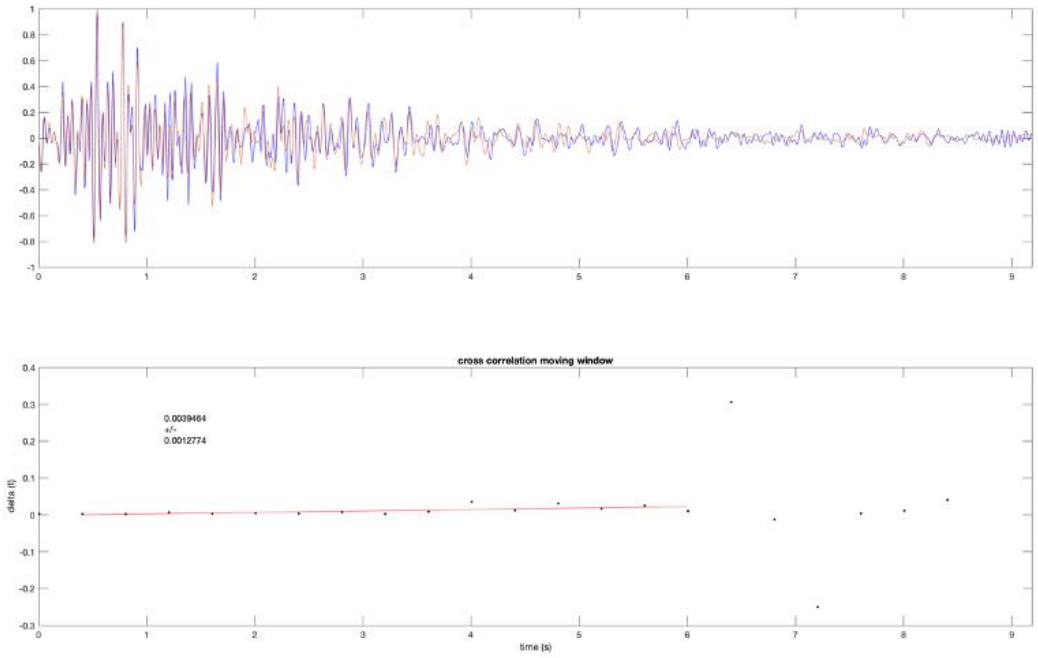

Figure 16b. Top: visual comparison early part and coda for the multiplets detected on 29/05/2018 (blue) and 25/06/2018 (red), SN04 station. Bottom: CWI analysis. The velocity variation can be retrieved from the slope of the time vs lag-time.

Using CWI we have detected both long and short term changes in velocity at Sierra Negra volcano during the pre-eruptive phase. Our results show a decrease in the subsurface seismic velocities at each station, with the results for station SN04 summarized in Table 1.
Seismic velocity variations are in general correlated with the surface deformation, however the causes of these pre-eruptive changes are not well understood and at this stage there is no clear link.

Table 1. Event times for multiplets detected at SN04 IGUANA station, given as Day/Months, and the velocity changes computed.

Event 1	**Event 2**	**Velocity Change, %**
25/05	22/06	-0.26 +/- 0.05 %
23/05	21/06	-0.01 +/- 0.10 %
29/05	25/06	-0.39 +/- 0.12 %
05/06	18/06	-0.15 +/- 0.08 %
05/06	25/06	-0.15 +/- 0.1 %
29/05	20/06	-0.12 +/- 0.03 %
30/05	23/06	0.006 +/- 0.03%
04/06	19/06	0.09 +/- 0.04 %

4. Seismic velocity changes in Iceland detected using ambient noise

IMO has in cooperation with the Royal Observatory of Belgium and Institut des Sciences de la Terre (ISTerre, France) studied seismic velocity changes in volcanic regions of Iceland using continuous recordings of ambient seismic noise. This deliverable briefly describes the near-real time monitoring of the unrest around Mt. Thorbjörn that we performed during the 2020 repeated magmatic intrusions in the Reykjanes Peninsula, SW Iceland.

In late January 2020 a rapid magmatic intrusion was detected in the Reykjanes Peninsula, an oblique rift in the southwestern part of Iceland. The surface deformation, manifested as an uplift signal, was observed on GPS and InSAR and centered roughly 2 km west of Mt. Thorbjörn; 2 km NNW of seismic station GRV. Deformation studies indicated three different inflation periods over seven months (January-late July) and initial modeling of deformation data revealed thin and long sills located at ~4 km depth in the crust (M.M. Parks personal communication). At a similar time, an intense earthquake swarm started and in total approximately ~14,000 earthquakes (M>-2) were recorded from late January until late July around the center of the uplift. Five new seismic stations were installed in the area in January/February and in total ten seismic stations within a radius of 18 km from the center of uplift provided a good opportunity to study the effect of magmatic intrusions on seismic velocity changes. Figure 17 displays the distribution of seismic stations in the Reykjanes Peninsula in February and the region of uplift, which is indicated by a purple dashed rectangle.

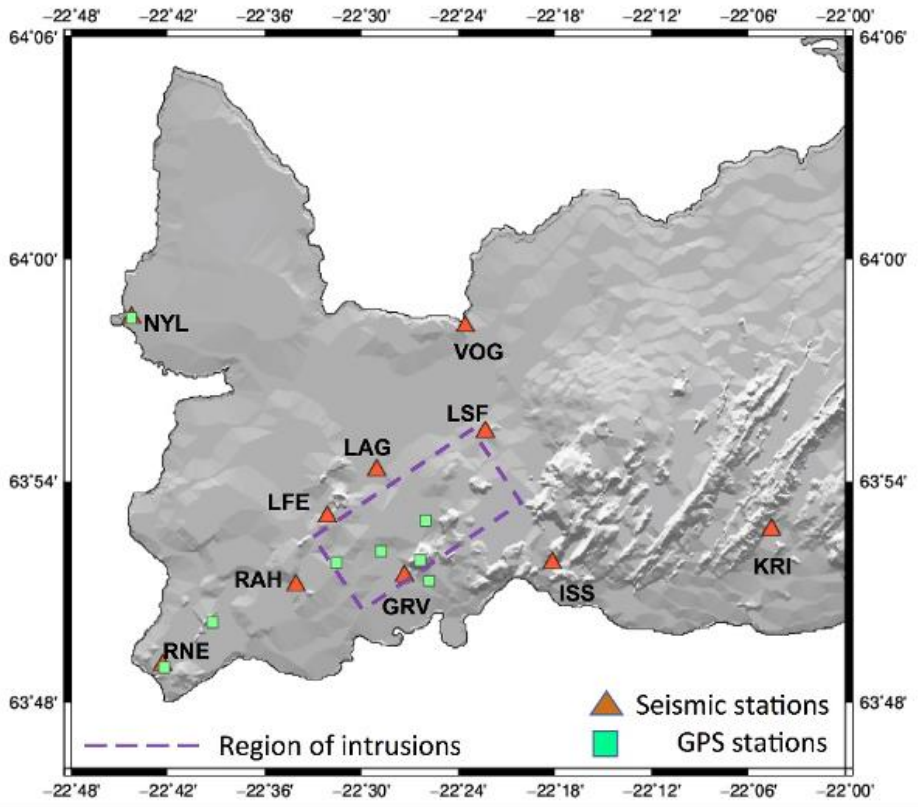

Figure 17. Map of the Reykjanes Peninsula showing seismic and GPS stations. The area showing signs of inflation is indicated with a purple dashed rectangle.

With the continuous seismic data being streamed to IMO, seismic velocity changes could be analyzed and even monitored on a daily basis. For our analyses we used the state-of-the-art MSNoise software

package (http://www.msnoise.org) to calculate cross-correlation functions (CCFs) of ambient seismic noise (Lecocq et al., 2014). We quantified the relative seismic velocity variations (dv/v) with seismic interferometry. MSNoise is a very effective python-based workflow tool developed for processing and organizing a large amount of seismic noise data. A schematic workflow of a sample MSNoise project is presented in Figure 18.

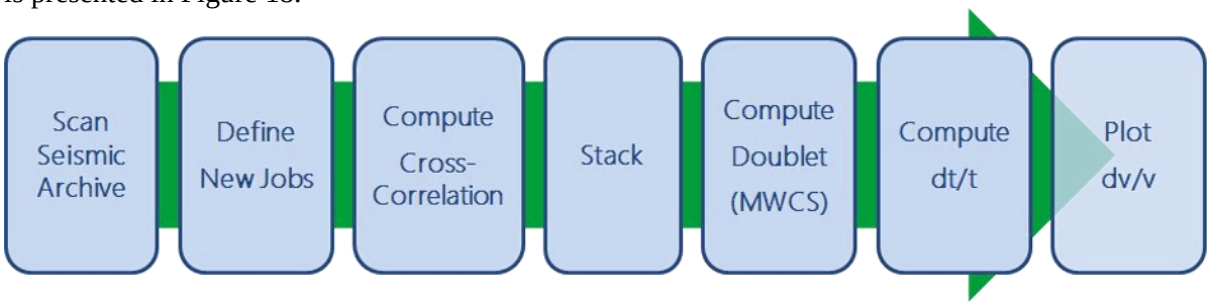

Figure 18. Schematic workflow of MSNoise displaying data processing steps starting from scanning the data archive, job selection, computation of CCFs and stacks, seismic velocity change measurement and plotting the results.

Our results show a significant decrease in the subsurface seismic velocities in the vicinity of Mt.Thorbjörn during the unrest period. Figure 19 displays a rapid dv/v decrease during the volcanic unrest period in all three-component-based cross-components (e.g., NZ, EZ, EN) for the GRV station (single station autocorrelation). After six months, temporal changes in dv/v tended to return to pre-unrest background levels. Seismic velocity variations are in general agreement with the deformation data, however there are more details in the dv/v time series which we cannot easily interpret at this point.

Figure 20 shows seismic velocity changes between two different stations using vertical component cross-correlation analyses and 4 different station pairs. The different frequency bands used can be interpreted as sensitivity towards different volumes in the crust and depths between the stations, where volume sensitivity increases for lower frequencies. We conclude that relative seismic velocity changes based on single station, cross component analyses of a close-range station give more reliable results than cross-correlation calculations of station pairs, probably due to high attenuation in the crust.

The outcomes of this work can be summarized as follows; (1) near-real-time delivery of dv/v results for following magmatic activity in the Reykjanes Peninsula (2) development of post-processing codes and visualizations tools (3) useful for informing the National Civil Protection of Iceland to assess this intrusive period and determine effective early warnings for possible hazards. This study of unrest on Reykjanes Peninsula is part of a larger national project, supported by the Icelandic Research Fund, RANNIS (Grant No: 185209-051).

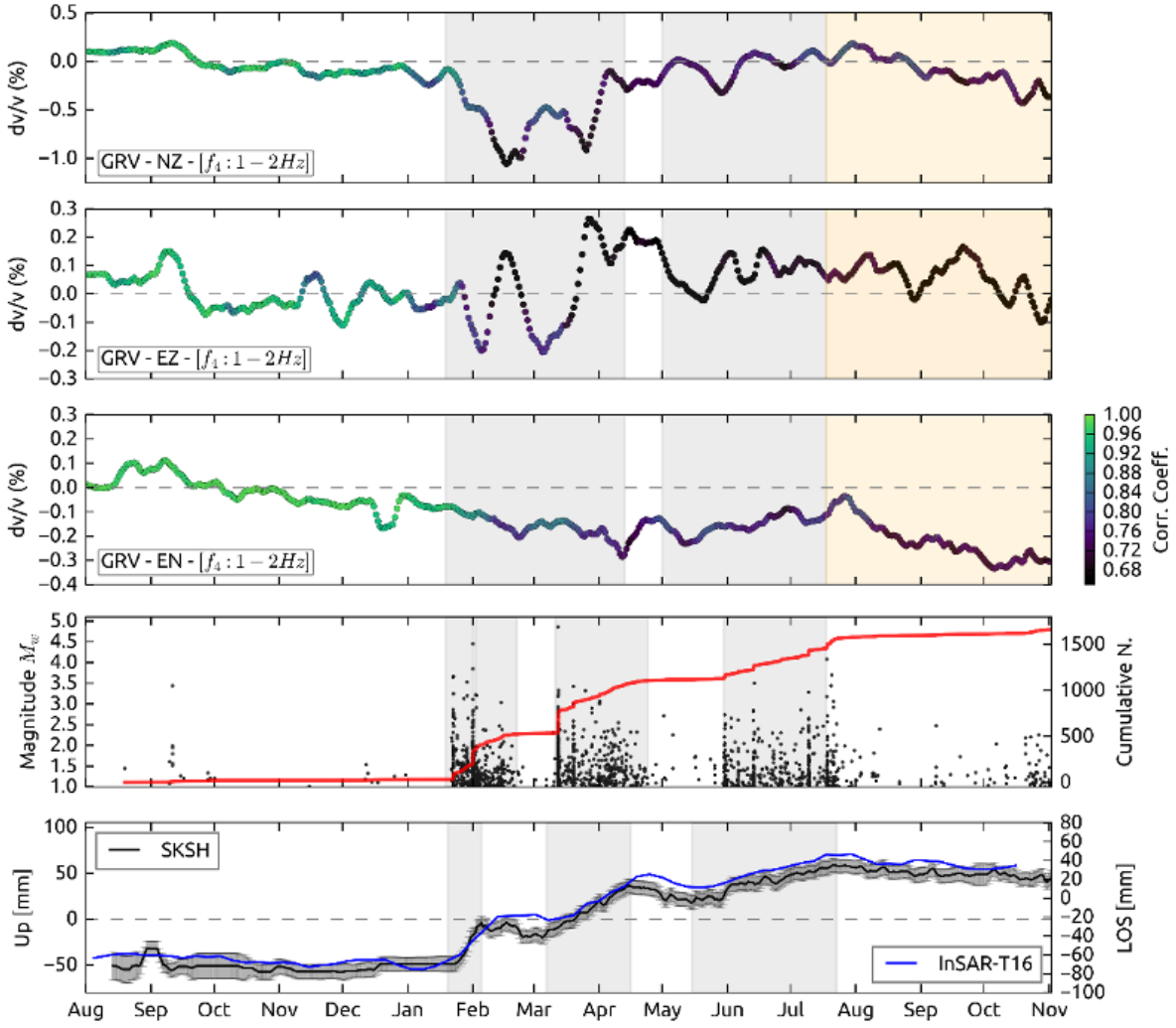

Figure 19. Seismic velocity changes for GRV seismic station. The gray boxes correspond to periods related to Mt.Thorbjörn inflation. The color scale displays the correlation coefficient. The bottom panel shows the time series of the uplift at GPS station SKSH and the LoS displacement obtained from InSAR (TSX)

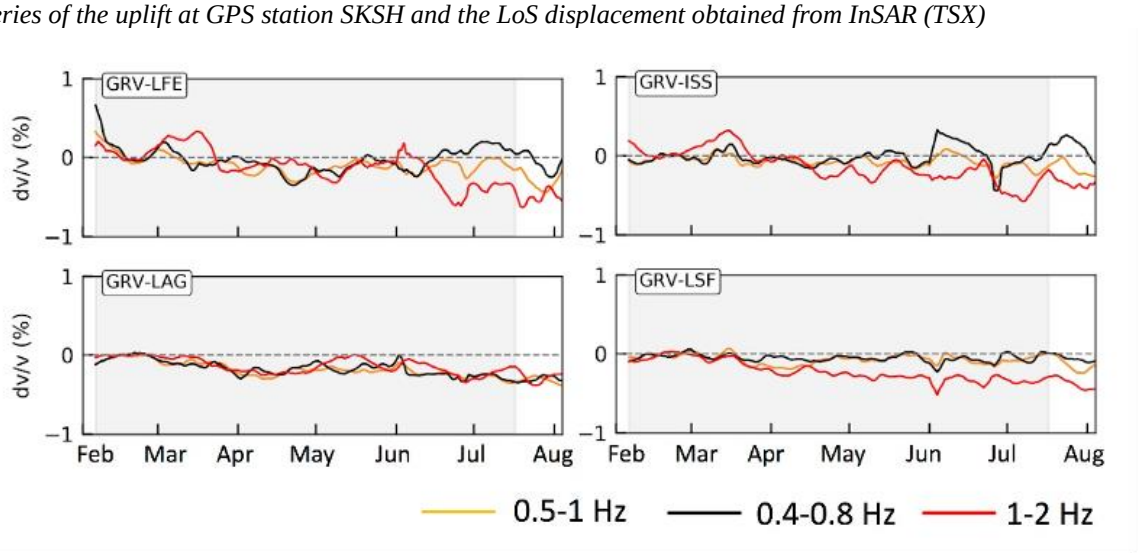

Figure 20. Seismic velocity changes using cross-correlations between different seismic station pairs. The calculated frequency ranges are color coded and displayed in the bottom of the figure.

5. Seismic velocity changes at El Hierro, Canary Islands in 2011-2014

Observations and modelling of the strain field will be undertaken as an aid to the interpretation of seismic wave velocity changes.

Our objective is studying crustal velocity variations that could occur in association with a magmatic process. For this purpose, we use seismic data (IGN, volcano monitoring network) collected during the unrest (2011), eruption (2011-2012) and further reactivation processes (2012-2014), that occurred in El Hierro Island (Canary Island, Spain) in the period 2011-2014. We address this objective by using different approaches:

1. Improving the seismic catalogue for the unrest period (19th July-10th October 2011): We developed a semi-automatic earthquake detection and location system to improve the completeness of the IGN seismic catalogue (approx. 10,000 events for the unrest period). First, a STA/LTA algorithm was applied to the power spectra of the signal optimizing the computation time to detect the earthquakes. Analyzing the power spectra instead of the waveforms increases substantially the number of events detected. Second, a matching- template algorithm (waveform correlation) with well-known earthquakes manually characterized as templates was used to pick seismic phases. The algorithm requires similar earthquakes during the swarm, something very likely to happen during volcanic unrest. The seismic event locations are achieved by applying the Hypoellipse software to the phases obtained from the matching template algorithm. As a preliminary result, up to 40,040 potential earthquakes have been detected. Moreover, using 3,500 earthquakes as a template we have applied a matching template algorithm. 35,000 potential earthquakes have been classified as earthquakes through phase picking, of which, we have been able to locate ~29,000 earthquakes using Hypoellipse.

2. We have analyzed the temporal variations in the P- (compressional) and S- (shear) wave travel-time velocities (Vp/Vs) using the new catalogue dataset for the unrest period. In volcanic areas, the Vp/Vs ratio allows the properties of the medium to be studied particularly the existence of fluids and/or increasing or changing crack distribution, thereby identifying the state of the volcano and its evolution. We have calculated the Vp/Vs ratio and Poisson's ratios by applying the Wadati method, using the phase information (P- and S-wave arrival times) of the located events and a robust multilinear regression for events with enough phase quality, <1.5 s residual. We show results in Figure 21.

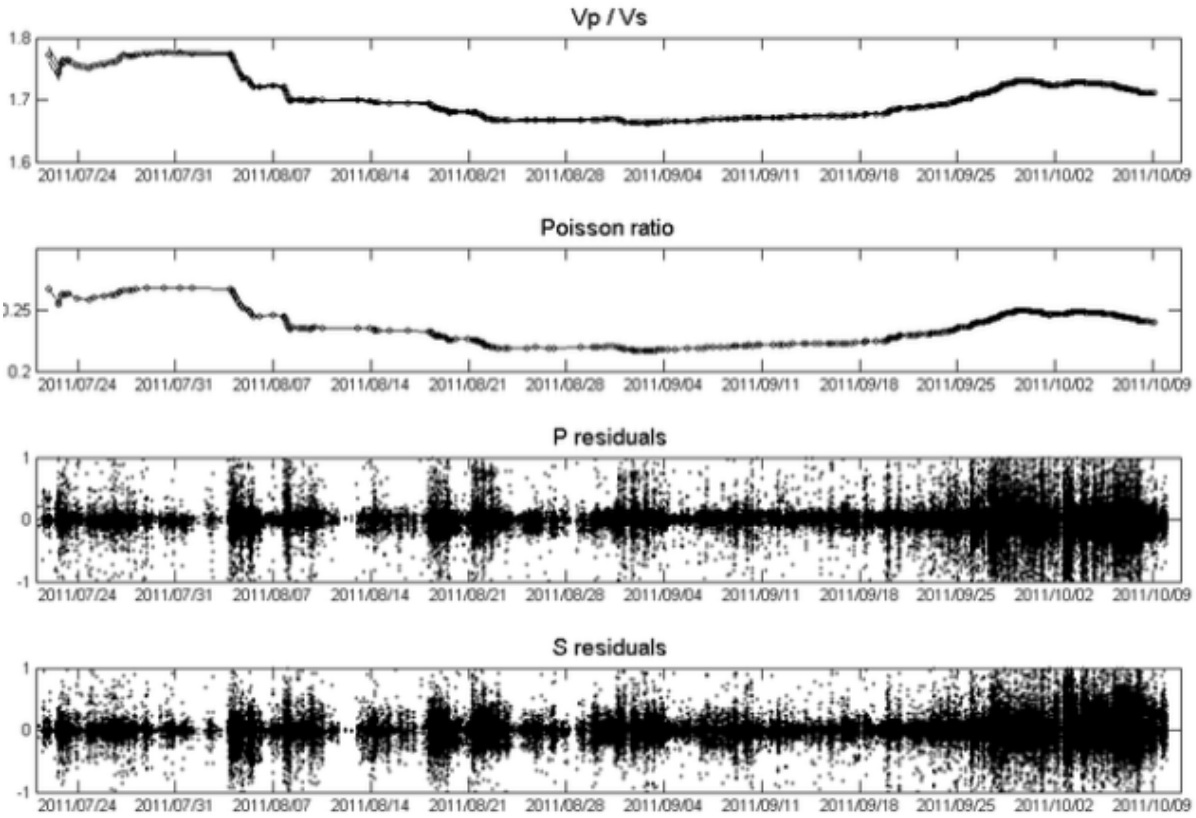

Figure 21. Time evolution of Vp/Vs, Poisson's ratio, and P and S residuals

3. We have applied variable Vp/Vs values in event relocation for the entire new catalogue, with the relocated events shown in Figure 22.

The locations obtained with Vp/Vs variations show slight differences with respect to the locations with a static Poisson coefficient. These differences are mainly observed in the panels (a,b) of Figure 22. It seems that the earthquake clusters are better defined, which is observed from the end of July to mid-August. Although there is no noticeable difference in the other coordinates, there is a slight difference in the depth. The increase in depth in the weeks prior to the eruption seems to be less pronounced when the time-varying Vp/Vs ground model is applied.

4. By using LOTOS software, we compare tomographic 3D velocity models obtained with the seismic catalogue covering the unrest period and the reactivation periods in order to check if a difference in media exists (Figure 23).

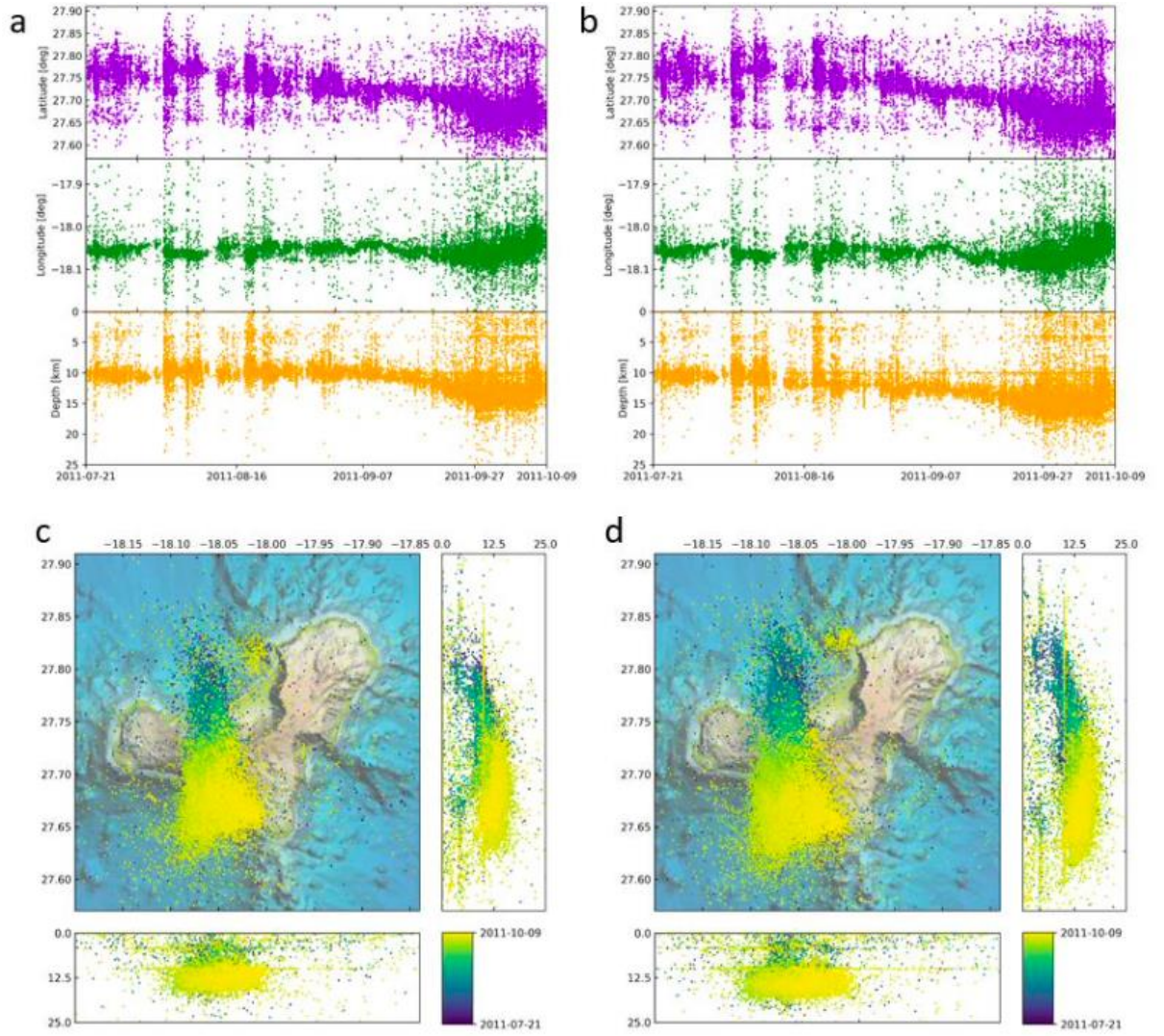

Figure 22. Catalogue relocation using time-varying Vp/Vs ratio. a) Time variation of Latitude, Longitude and Depth of the original catalogue and c) the epicentral and vertical distribution of the seismicity located during the unrest b) Latitude, Longitude and Depth time variations of the new catalogue applying time varying Vp/Vs values, and d) the epicentral and vertical distribution of the seismicity located during the unrest.

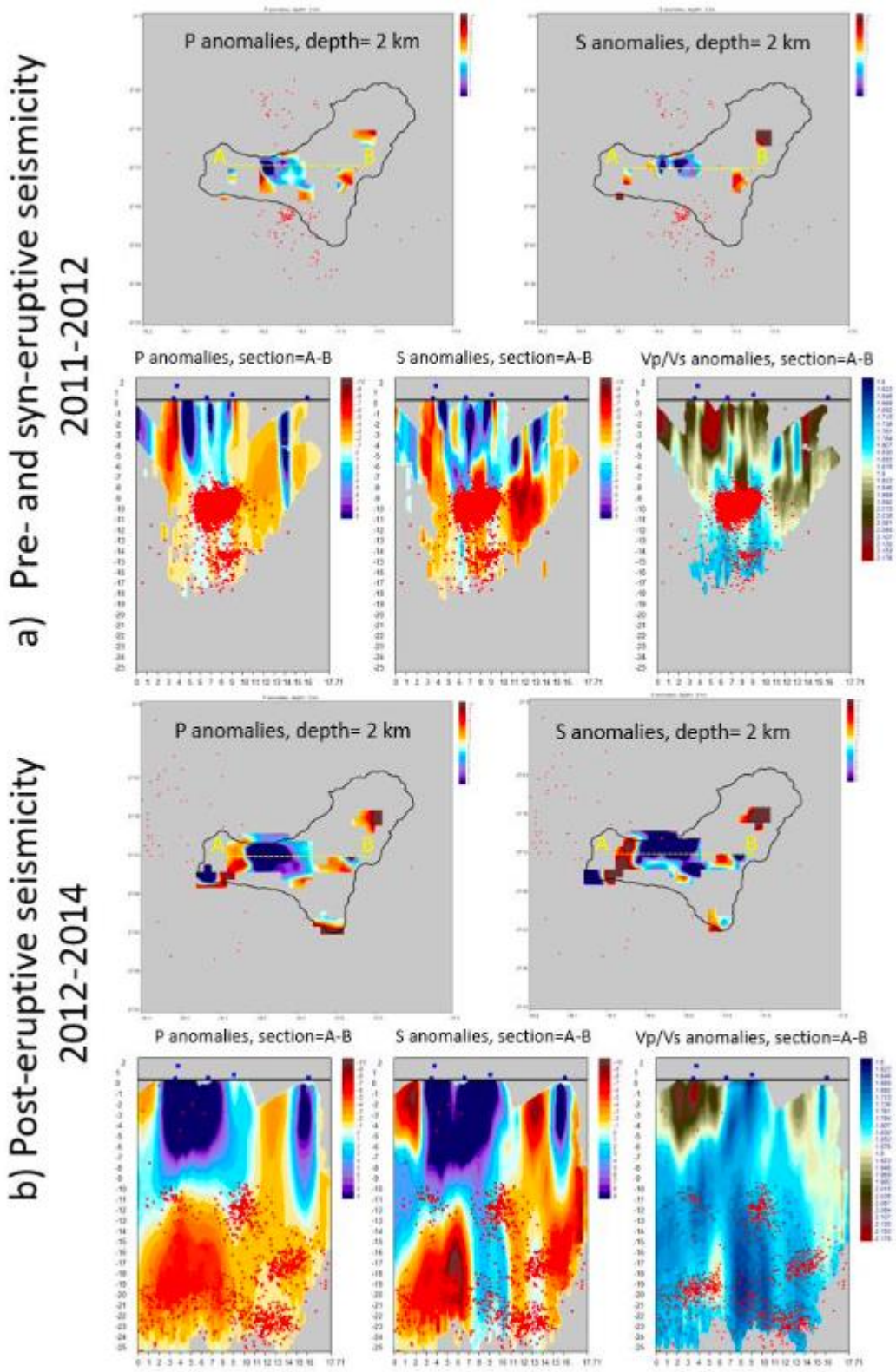

Figure 23. Ground P and S velocity models comparison. a) P and S velocity anomalies at depth=2km, P, S and Vp/Vs anomalies for a vertical section (A-B), obtained by tomographic inversion using the new catalogue for the unrest period and the syn-eruptive seismicity. b) P and S velocity anomalies at depth=2km, P, S and Vp/Vs anomalies for a vertical section (9A-9B), obtained by tomographic inversion using the post-eruptive activity located in El Hierro.

Preliminary results suggest the occurrence of changes in seismic P and S wave velocity, before and after the eruptive activity occurred in El Hierro, with on average, greater Vp/Vs values during unrest in comparison with the post-eruptive period.

As future work we will address the study of additional parameters associated with the changes in the stress field (attenuation, Shear-wave splitting) to check the consistency and validity of the preliminary results. We will also study the consequences of varying the state parameters in the inversion of the pressure sources, using the GNSS deformation time series associated with this eruptive event.

6. Joint inversion of multiparametric data

University of Iceland (UI), together with Icelandic Meteorological Office (IMO) and University of Leeds (ULeeds), has carried out work towards Task 9.6 by developing a new approach for joint inversion of multiparametric data. The primary objective of this task is to develop data driven tools to automate the diagnosis of volcanic state variations in real-time (to be reported in D9.3). The UI work is reported in a recent paper in Nature Communications (Sigmundsson et al., 2020). The study sheds light on what conditions need to be in place in a volcano for an eruption to start; a prerequisite for work on Task 9.6.

One important factor not fully considered before in many models applied to geodetic data, is the role of magma buoyancy. Magma may be less dense than the host rock surrounding it. Where magma accumulates in volcano roots it can therefore have a large upward directed buoyancy force. This means that if sufficient magma accumulates, this force can be an important component of the overall force necessary to break the surrounding host rock so magma can flow upwards. This is inferred to have been the case for the Bárdarbunga 2014-2015 unrest in Iceland and associated Holuhraun eruption, when precursors (Figure 24) prior to failure of the magma body responsible for this largest eruption in Iceland in 200 years were “mild” (small increase in seismicity in last several months prior to magma body failure; small detected ground displacement), and much less than for many other eruptions in Iceland in recent decades. An implication of the work is that large eruptions can occur with only minor precursory activity. This needs to be considered in Task 9.6.

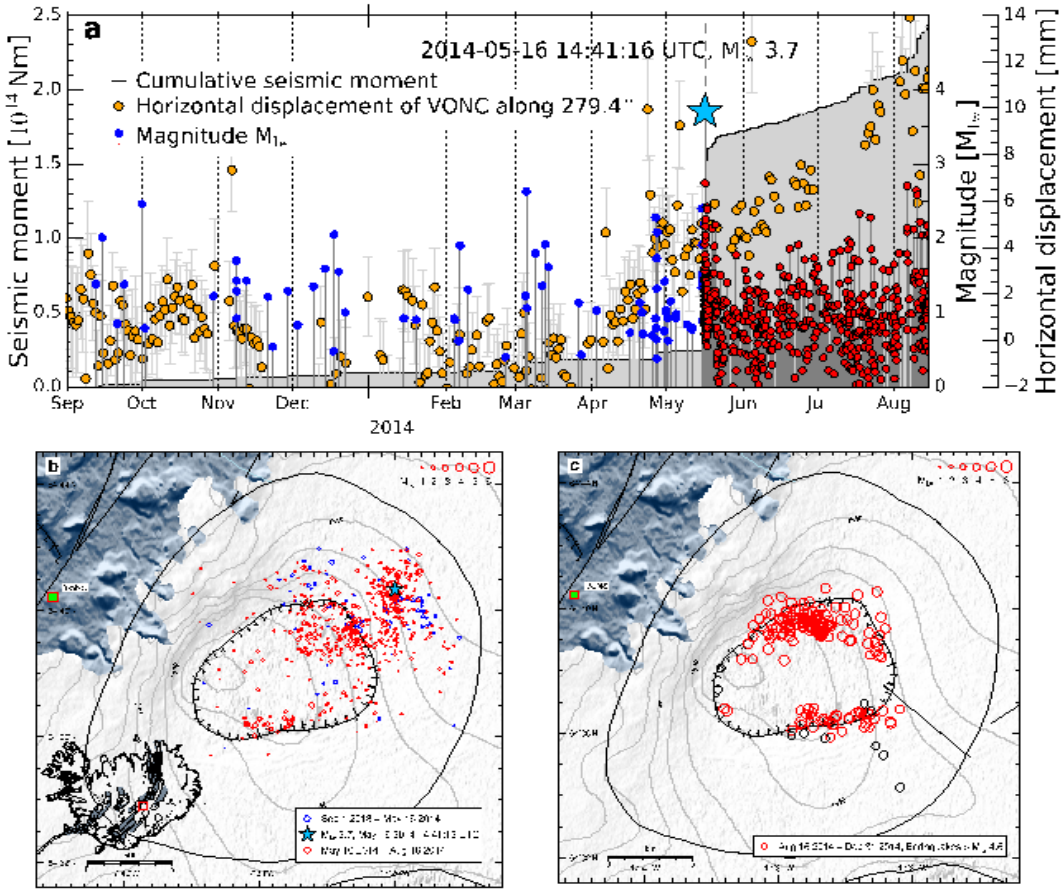

Figure 24. Seismicity and deformation at Bárdarbunga. ***a****, Earthquakes versus time (1 September 2013 – 14 August 2014; before diking and eruption) plotted as impulses scaled with magnitude (right axis). Earthquakes prior to the M3.7 event on 16 May 2014 shown in blue and red afterwards. Also shown is cumulative seismic moment (shaded in grey; left axis), and horizontal displacement in direction 283.5º (yellow dots) at GPS-station VONC from detrended time series. Error bars in grey.* ***b****, Inferred location of the earthquakes shown in* ***a****, with earthquakes prior to M3.7 event on 16 May 2014 shown in blue and red afterwards. Small map of Iceland shows the study area outlined with a red box, and fissure swarms with grey shading.* ***c****, Location of M>4.6 earthquakes during the caldera collapse. Note aseismic segments of the caldera. Background map shows Vatnajökull ice cap in white, and outlines of the Bárdarbunga central volcano (oval shape) and its caldera. Straight lines show segments of the lateral dike that formed; black open circles are ice cauldrons.*

References

Cubuk-Sabuncu, Y., Caudron, C., Lecocq, T., Jonsdottir, K., Parks, M.M., Mordret, A., Geirsson, H., Temporal seismic velocity changes during the 2020 rapid inflation at Mt.Thorbjörn, Iceland, using seismic ambient noise (in prep).

De Angelis, S., Haney, M.M., Lyons, J.J., Wech, A., Fee, D., Diaz-Moreno, A., et al. (2020). Uncertainty in Detection of Volcanic Activity Using Infrasound Arrays: Examples From Mt. Etna, Italy. Frontiers in Earth Science 8, 169.

Eibl, Eva P. S., Bean, C.J., Vogfjörd, K.S., Ying, Y., Lokmer, I., Möllhoff, M., O'Brien, G.S., & Pálsson, F. (2017). Tremor-rich shallow dyke formation followed by silent magma flow at Bárðarbunga in Iceland. Nature Geoscience volume 10, pages 299–304

Geirsson, H., P. LaFemina, T. Árnadóttir, E. Sturkell, F. Sigmundsson, M. Travis, P. Schmidt, B. Lund, S. Hreinsdóttir, and R. Bennett (2012), Volcano deformation at active plate boundaries: Deep magma accumulation at Hekla volcano and plate boundary deformation in south Iceland, J. Geophys. Res., 117, B11409, doi:10.1029/2012JB009400.

Gibbons, S.J., Schweitzer, J., Ringdal, F., Kværna, T., Mykkeltveit, S., and Paulsen, B. (2011). Improvements to Seismic Monitoring of the European Arctic Using Three-Component Array Processing at SPITS. Bulletin of the Seismological Society of America 101(6), 2737-2754.

Haney, M.M., Van Eaton, A.R., Lyons, J.J., Kramer, R.L., Fee, D., and Iezzi, A.M. (2018). Volcanic Thunder From Explosive Eruptions at Bogoslof Volcano, Alaska. Geophysical Research Letters 45(8), 3429-3435. doi: 10.1002/2017GL076911.

Hotovec-Ellis, A.J., and Jeffries, C., (2016). Near Real-time Detection, Clustering, and Analysis of Repeating Earthquakes: Application to Mount St. Helens and Redoubt Volcanoes – Invited, presented at Seismological Society of America Annual Meeting, Reno, Nevada, 20 Apr.

Johannes Schweitzer, J., J. Fyen, S. Mykkeltveit, S. J. Gibbons, M. Pirli, D. Kühn, and T. Kværna (2012). Seismic Arrays. - In: Bormann, P. (Ed.), New Manual of Seismological Observatory Practice 2 (NMSOP-2), Potsdam : Deutsches GeoForschungsZentrum GFZ, 1-80.
https://doi.org/10.2312/GFZ.NMSOP-2_ch9

Lecocq T., Caudron C. and Brenguier F., (2014). MSNoise: a python package for monitoring seismic velocity changes using ambient seismic noise Seismol. Res. Lett. 85 715–26

Ófeigsson, B. G., A. Hooper, F. Sigmundsson, E. Sturkell, and R. Grapenthin (2011), Deep magma storage at Hekla volcano, Iceland, revealed by InSAR time series analysis, J. Geophys. Res., 116, B05401, doi:10.1029/2010JB007576.

Olson, J.V., and Szuberla, C.A.L. (2005). Distribution of wave packet sizes in microbarom wave trains observed in Alaska. The Journal of the Acoustical Society of America 117(3), 1032-1037. doi: 10.1121/1.1854651.

Schweitzer, J., M. Roth (2015), Biannual Report prepared for the FDSN Meeting during IUGG General Assembly in Prague, 2015, 14 pp.
https://www.fdsn.org/media/meetings/2015/NORSAR_Network_Report.pdf

Sigmundsson, F., Pinel, V., Grapenthin, R., Hooper, A., Halldórsson, S.A., Einarsson, P., Ófeigsson, B. G., Heimisson, E. R., Jónsdóttir, K., Gudmundsson, M.T., Vogfjörð, K., Parks, M., Li, S., Drouin, V., Geirsson, H., Dumont, S., Fridriksdottir, H. M., Gudmundsson, G. B., Wright, T., Tadashi Yamasaki, T. (2020), Unexpected large eruptions from buoyant magma bodies within viscoelastic crust, Nature Communications, 11, 2403.

Smith, P. J. and Bean, C. J., (2020), RETREAT: A REal-Time TREmor Analysis Tool for Seismic Arrays, With Applications for Volcano Monitoring. Front. Earth Sci. 8:586955. doi: 10.3389/feart.2020.586955

Snieder R. (2006). The Theory of Coda Wave Interferometry. Pure Appl. Geophys., 163, 455-473. doi: 10.1007/s00024-005-002-6.